



**HAL**  
open science

# Using discrete systems to exhaustively characterize the dynamics of an integrated ecosystem

Cedric Gaucherel, Franck Pommereau

► **To cite this version:**

Cedric Gaucherel, Franck Pommereau. Using discrete systems to exhaustively characterize the dynamics of an integrated ecosystem. *Methods in Ecology and Evolution*, 2019, 10 (9), pp.1615-1627. 10.1111/2041-210X.13242 . hal-02265554

**HAL Id: hal-02265554**

**<https://hal.science/hal-02265554>**

Submitted on 11 Oct 2019

**HAL** is a multi-disciplinary open access archive for the deposit and dissemination of scientific research documents, whether they are published or not. The documents may come from teaching and research institutions in France or abroad, or from public or private research centers.

L'archive ouverte pluridisciplinaire **HAL**, est destinée au dépôt et à la diffusion de documents scientifiques de niveau recherche, publiés ou non, émanant des établissements d'enseignement et de recherche français ou étrangers, des laboratoires publics ou privés.

1 Standard paper:

2

3

# Using discrete systems to exhaustively characterize the dynamics of an integrated ecosystem

5

6

7

Gaucherel C. <sup>(1)\*</sup>, Pommereau F. <sup>(2)</sup>

8

<sup>1</sup> AMAP - INRA, CIRAD, CNRS, IRD, Université Montpellier, Montpellier, France

9

<sup>2</sup> IBISC, Université d'Evry-val d'Essonne, Université Paris-Saclay 91025 Evry, France

10

11

Correspondence to:

12

\* Cédric Gaucherel

13

INRA – EFPA, UMR AMAP, TA A.51/PS2, 34398 Montpellier Cedex 5 (France)

14

Tel.: 33 (0)4 67 61 65 86

15

Fax: 33 (0) 4 67 61 56 68

16

Email: [gaucherel@cirad.fr](mailto:gaucherel@cirad.fr)

17

18

Word count: 6352      Running head: Ecosystem dynamics viewed by Petri nets.

19

Published as: Gaucherel, C, Pommereau, F. Using discrete systems to exhaustively characterize the dynamics of an integrated ecosystem. *Methods Ecol Evol.* 2019; 10: 1615– 1627.

20

21

<https://doi.org/10.1111/2041-210X.13242>

## 22 Abstract

23 1. To understand long-term ecosystem dynamics, several concepts have recently been proposed  
24 that consider ‘basins of attraction’ used to express resilience, and ‘tipping points’ that express  
25 sharp change in an ecosystem’s behavior. However, these temporal features remain difficult to  
26 identify and quantify, because current models usually only focus on a part of the whole  
27 ecosystem behavior, whereas a holistic approach should be preferred.

28 2. We propose an original family of models based on discrete systems and designed to  
29 comprehensively characterize ecosystem dynamics holistically and over the long term. We  
30 developed a qualitative model based on Petri nets, made up of a relational graph (interaction  
31 network) that was then rigorously handled using transition rules. Unlike traditional modelling  
32 and graph theory approaches, transition rules can strongly modify the graph structure (i.e. a  
33 dynamic topology occurs).

34 3. We examined the value of Petri nets when applied to the simple ecosystem of a termite colony.  
35 A termite colony comprises abiotic and biotic components and processes that we explored along  
36 all of their possible trajectories.

37 4. Several temporal features were easily detected and quantified, such as basins of attraction (i.e.  
38 strongly connected states), tipping points (critical transitions along trajectories) and various kinds  
39 of collapses (functioning systems whose structures were nevertheless fixed). We propose that  
40 Petri nets developed for more complex ecosystems will provide original insights into their holistic  
41 behavior.

42

43 Keywords: ecosystem resilience; ecosystem collapse; integrated model; discrete systems;  
44 formalization.

45

## 46 Introduction

47 The concept of resilience is used to describe an ecosystem when it persists in the face of  
48 perturbations (Holling 1973; DeAngelis 1980; Scheffer 2009). This concept is the subject of continued  
49 debate, with several ongoing definitions, although most ecologists acknowledge its relevance to  
50 understanding ecosystem dynamics. While easily understandable, the concept of resilience remains  
51 difficult to quantify and predict (Walker *et al.* 2004; Hirota *et al.* 2011; Karssenberg, Bierkens &  
52 Rietkerk 2017). Recently, a conceptual view has been put forward to represent the richness of  
53 ecosystem dynamics. This approach proposes to plot the parameter zones in which the system is  
54 considered to be resilient, as 'basins of attraction' or 'wells,' whose depth is said to quantify the  
55 intensity of resilience (Scheffer *et al.* 2001; Scheffer *et al.* 2015). It is now necessary to develop the  
56 most appropriate methods to determine the behavior of these basins of attraction, therefore a new  
57 type of model needs to be developed for this purpose.

58 An ecosystem can possess several potential basins between which it can alternate (Thom 1975;  
59 Gaucherel 2010). Consequently, the system possesses a range of possible trajectories, within or  
60 between these basins, that are considered relatively stable zones, i.e., where the system is more  
61 frequently found. When the system shifts from one basin to another, it is said to cross a tipping point  
62 (TP) or a catastrophic shift (Scheffer *et al.* 2001; Hirota *et al.* 2011). Several studies have shown that  
63 ecosystems and environmental systems experience sharp TPs (Scheffer *et al.* 1993; Carpenter 2003),  
64 over the short and/or long term (Hély *et al.* 2009; Lenton *et al.* 2012). However, TPs, like the  
65 resilience to which they are connected, are notoriously difficult to identify and quantify. It is  
66 therefore critical to correctly identify: i) the basins of attraction of an ecosystem, ii) basin depth, and  
67 iii) the relative locations of these basins in the potential landscape, if we are to deduce the possible  
68 TPs linking basins to each other (Walker *et al.* 2004; Scheffer *et al.* 2015).

69 Several models have been proposed to describe resilience and tipping points in various systems. The  
70 pioneering approach in this field was the catastrophe theory developed by (Thom 1975). Thom

71 (1975) created powerful yet hard-to-handle algebraic tools to analyze and understand the potential  
72 of any system. In ecology, the common model used is usually a one dimensional ordinary differential  
73 equation handling the central state-variable (e.g. biomass, Scheffer *et al.* 2001; Van Nes & Scheffer  
74 2007). The direct consequences of using such equations are that they focus on the dominant  
75 behaviour in a system and reduce the study to a fixed phase-space defined by the state-variables.  
76 Conversely, more rare trajectories can occur, and most catastrophes may even require a qualitative  
77 shift in the system variables as well as in the phase-space (Thom 1975; Hély *et al.* 2019). For example,  
78 a shift from a forest to a grassland state will drastically change its vegetation composition, fire  
79 regime, faunal communities and trophic network (Hély *et al.* 2009; Hély *et al.* 2019). Tipping points  
80 will disrupt the entire system structure and functioning, and therefore should be examined using  
81 models dedicated to exhaustive behavior analysis.

82 To model a rapidly changing ecosystem, we developed a method using Petri nets, which have been  
83 used successfully in theoretical computer science and systems biology (Pommereau 2010; Reisig  
84 2013). Petri nets are similar to Boolean networks (Kauffman 1969; Thomas & Kaufman 2001), as they  
85 are well adapted to formalize network topological changes. To our knowledge, such discrete and  
86 qualitative models have rarely been used in ecology (but see Ewing *et al.* 2002; Cordier, Largouët &  
87 Zhao 2014; Baldan *et al.* 2015; Gaucherel *et al.* 2017). Among discrete models, Petri nets are  
88 powerful tools that enable the rigorous formalization of exhaustive changes in an ecosystem's  
89 structure. Petri nets can be used to scrutinize all possible fates of a system and to map every  
90 potential qualitative trajectory. Although qualitative, it is nevertheless possible to compute  
91 quantitative metrics from the model outputs and deduce many system properties (Koch, Reisig &  
92 Schreiber 2011).

93 We examine the potential of Petri nets to model a simple ecosystem. Our objective is to manipulate  
94 an ecosystem-like structure, composed of biotic and abiotic (and anthropogenic-like) components  
95 working in close interaction, with potential disturbances occurring (Turner 2009; Gaucherel *et al.*

96 2017). Therefore, we chose to model a (Macrotermitinae) termite colony, because a full termite  
97 colony develops from reproductives (queen and king) and external resources, and can drastically shift  
98 into a different system when experiencing strong disturbance, e.g., mound destruction or attack. The  
99 termite colony could then reach a collapsed (or deadlock) state via various trajectories. We need a  
100 rigorous, formalized model to confidently identify resilience zones, such as basins of attraction, the  
101 tipping points separating them, and possibly other properties of system behavior such as collapse.

102

## 103 [Materials and methods](#)

### 104 [Case study - a eusocial insect ecosystem](#)

105 Eusociality is characterized by cooperative brood care, overlapping adult generations, and division of  
106 labor between castes that leads to reproductive and sterile groups (Costa & Fitzgerald 2005). We  
107 chose to model eusocial insect colonies for their propensity to experience drastic changes (tipping  
108 points) over time, but any other ecosystem-like models may be used. We chose to work on  
109 Macrotermitinae termites, which construct large colonies (up to millions of inhabitants, Fowler *et al.*  
110 1986), (Turner 2009) . Termites cultivate fungi in special chambers, build aerial structures (called  
111 mounds) to improve air circulation, and divide each nest into a royal chamber, fungus chambers, and  
112 egg rooms (Fig. 1a, Suppl. Mat. Appendix 1). Given the ability for this eusocial species to produce  
113 fungi, termites might also be considered as mimicking agricultural (farmer) activities. One way of  
114 conceptualizing the ecosystem under study is to represent it as a network of elements in interaction  
115 (Fig. 1b). This *ecosystem graph* is then handled by the following model.

### 116 [Petri nets](#)

117 We propose a twofold approach: i) first, the interaction network of the ecosystem is represented by  
118 a graph designed to gather any kinds of ecological processes (not to be confused with purely trophic,

119 pollinator or parasitic networks, Thébault & Fontaine 2010; Campbell *et al.* 2011); ii) second, a  
120 rigorous model based on a Petri net is developed to formalize any change in the graph topology (i.e.  
121 neighboring relationships). Petri nets, developed in computer sciences (Pommereau 2010; Reisig  
122 2013) and also used in systems biology (Murata 1989; Blätke, Heiner & Marwan 2011; Koch, Reisig &  
123 Schreiber 2011), are powerful tools for rigorously formalizing changes in network topologies  
124 occurring during the system dynamics. The two major differences between a Petri Net model and  
125 other network models used in ecology (Thébault & Fontaine 2010; Kéfi *et al.* 2016) are that Petri net  
126 models deal with *topological changes during* simulations and can explore all possible dynamics of the  
127 system. Although the maximal interaction network remains predefined in our study, it is continuously  
128 modified within runs and any drastic changes are fully controlled (Gaucherel *et al.* 2017). These  
129 differences therefore make our model difficult to compare to existing models. For example, a  
130 predator-prey model would focus only on one ecosystem state of the dynamics produced. Such  
131 discrete models provide convenient and commonly used tools to exhaustively analyze the states of  
132 the system (called the state-space), the relatively stable (resilient) zones, the tipping points and any  
133 system trajectory (Walker *et al.* 2004; Scheffer *et al.* 2015). In this section, we start by presenting a  
134 simplistic predator-prey model and we then define multisets required to rigorously define Petri nets  
135 that will then be used to model the termite colony.

### 136 [A simplistic predator-prey Petri net](#)

137 We first illustrate Petri nets with a simplistic but unrealistic predator-prey system. In the predator-  
138 prey system, only two nodes are defined as the prey and predator populations (these are not  
139 individuals, Fig. 2a). The state of the system is defined by the set of "+" and "-" nodes, graphically  
140 drawn as having a token (a mark) or not, representing the presence and absence of each system  
141 component, respectively (see next section for a formal definition). The maximal number of possible  
142 system states is  $2^{\text{\#nodes}}$  and grows exponentially with the node number. The state of a node depends  
143 on the node states to which it is connected, while a connection between nodes exists as soon as one  
144 process makes this connection explicit (Fig. 2b). The rules correspond to any physicochemical,

145 biological and ecological and/or human-like processes (or sub-processes), and thus represent all  
146 interactions between nodes composing the ecosystem studied. In the predator-prey system, only  
147 two rules are defined: R1, the predation itself, and R2, the mortality (Fig. 2b).

148 In the formalism of this ecosystem, a rule is made up of condition and realization parts written by  
149 convention as: “transition’s name: condition  $\rightarrow$  realization”. In the predator-prey system, the rules  
150 are written as R1: P+, N+  $\rightarrow$  N- and as R2: N-, P+  $\rightarrow$  P-, with P and N the predator and prey  
151 populations, respectively. Since the rules modify node states, they also change the system state.  
152 Therefore, the system will shift from one state to another one through the successive applications of  
153 rules (Fig. 2b). These rules can then be translated into a Petri net in which the nodes are translated to  
154 pairs of *places*, and the rules are translated to *transitions*, both being connected through oriented  
155 *arcs* (Fig. 2c). Such a Petri net has its own dynamics: a transition that has enough tokens in its input  
156 places (those for which an arc exists from the input place to the transition) may *fire* (trigger),  
157 consuming tokens in its input places and producing new tokens in its output places (those for which  
158 an arc exists from the transition to the input place). These dynamics of the Petri net produce the  
159 *state space*, which provides the set of all system states reachable by the rules defined (Fig. 2d). As a  
160 corollary, the states are also connected to each other by some of these rules in the state space. The  
161 size of the state space is usually much smaller than the number of possible system states, because  
162 the computation starts from a specific initial condition and because rules have specific application  
163 conditions.

## 164 Formal definition of Petri nets

165 We now give a rigorous definition of Petri nets. To this end, we first need to define a *multiset* over a  
166 set  $X$  as a function  $\mu: X \rightarrow \mathbb{N}$ . We denote by  $X^*$  the set of all the multisets over  $X$ . A multiset  $\mu \in X^*$   
167 can be extended to a larger set  $Y \supset X$  by defining  $\mu(y) \stackrel{\text{def}}{=} 0$  for all  $y \in Y \setminus X$ . Given  $\mu_1$  and  $\mu_2$  in  $X^*$ ,  
168 we define:

- 169 • the sum of  $\mu_1$  and  $\mu_2$  by  $(\mu_1 + \mu_2)(x) \stackrel{\text{def}}{=} \mu_1(x) + \mu_2(x)$  for all  $x \in X$ ;

- 170 • the comparison of  $\mu_1$  and  $\mu_2$  by  $\mu_1 \leq \mu_2$  iff  $\mu_1(x) \leq \mu_2(x)$  for all  $x \in X$ ;
- 171 • the difference of  $\mu_1$  and  $\mu_2$  by  $(\mu_1 - \mu_2)(x) \stackrel{\text{def}}{=} \max(0, \mu_1(x) - \mu_2(x))$  for all  $x \in X$ ;
- 172 • the product by  $k \in \mathbb{N}$  by  $(k \times \mu)(x) \stackrel{\text{def}}{=} k \times \mu(x)$  for all  $x \in X$ .

173 Multisets may be denoted in extended sets notation as  $\mu = \{a, a, b\}$  that is such that  $\mu(a) = 2$ ,  
 174  $\mu(b) = 1$  and  $\mu(c) = 0$  for all  $c \notin \{a, b\}$ . A subset of a set  $X$  may be considered as a multiset by  
 175 identifying it to its characteristic function.

176 A *marked Petri net* is a tuple  $N \stackrel{\text{def}}{=} (S, T, W, M)$  such that:

- 177 •  $S$  is the finite set of *places*;
- 178 •  $T$ , disjoint from  $S$ , is the finite set of *transitions*;
- 179 •  $W: (S \times T) \cup (T \times S) \rightarrow \mathbb{N}$  is the weight function that defines *arcs*;
- 180 •  $M \in S^*$  is the *marking*, a multiset of places representing the state of the Petri net (the  
 181 number of tokens stored in each place).

182 Petri nets are commonly depicted as graphs (Fig. 2c), whose nodes are places (depicted as round-  
 183 shaped nodes) and transitions (square-shaped nodes), and whose edges are the arcs connecting  
 184 them with non-zero weight (*i.e.*, an arc drawn as  $x \rightarrow y$  is labeled by  $W(x, y) > 0$ , with 1 usually  
 185 omitted if  $W(x, y) = 1$ ), and the marking is depicted as black tokens  $\bullet$  within places (or the number  
 186 of tokens when this is more readable). An arc from a place to a transition (or conversely from a  
 187 transition to a place) is called an *input* (conversely *output*) arc (Fig. 2c). A pair of input/output arcs  
 188 with the same weights and between the same place and transition may be replaced by a single arc  
 189 with one arrow at each end (like the arcs connected to  $Ac^+$  in Fig. 3b).

190 For every transition  $t \in T$ , we define  $\vec{t} \stackrel{\text{def}}{=} \sum_{s \in S} W(s, t) \times \{s\} \in S^*$  and  $\overleftarrow{t} \stackrel{\text{def}}{=} \sum_{s \in S} W(t, s) \times \{s\} \in S^*$ .

191 For instance, we have  $\overleftarrow{R1} = \{N+\}$ , and  $\overrightarrow{R1} = \{P+, N-\}$  in Fig. 2c.

192 Let  $N \stackrel{\text{def}}{=} (S, T, W, M)$  be a marked Petri net. A transition  $t \in T$  is *enabled* at marking  $M$  iff  $\vec{t} \leq M$ . In  
 193 such a case,  $t$  may be *fired* yielding a new marking  $M' \stackrel{\text{def}}{=} M - \vec{t} + \overleftarrow{t}$ , which is denoted by  $M[t \rangle M'$ .

194 The *marking graph* (also called the reachability graph) of  $N$  is the smallest graph  $[ N ] \stackrel{\text{def}}{=} (V, E)$  such  
195 that  $M \in V$  and for all  $M' \in V$  such that  $M' [ t ] M''$  for a transition  $t \in T$ , then we also have  $M'' \in V$   
196 and  $(M', t, M'') \in E$ . Here,  $V$  stands for vertices (nodes) and  $E$  for edges. As an example, the marking  
197 graph of the predator-prey Petri net depicted in Fig. 2a is shown in Fig. 2d.

198 Essentially, a Petri net models the possible states of a system and the possible transitions between  
199 them, while the Petri net marking additionally uses tokens to indicate which state the system is  
200 currently in.

201

## 202 Results

### 203 Formal definition of a termite colony ecosystem

204 We modelled a termite colony as an ecosystem made up of biotic and abiotic components.  
205 Therefore, we defined an interaction network (i.e. a relational graph between system components)  
206 connecting nodes of various natures, with edges modelling various interactions and processes (Fig.  
207 1b, Appendix 1). A system node could belong to any one of the five categories: the permanent  
208 environment outside the colony (plotted in orange), resources (green), spatial structures (violet),  
209 inhabitants (blue), and competitors/predators (black) (Figure 1). A node could only take either one or  
210 the other of two Boolean states (Gaucherel *et al.* 2017): *On* or + (presence of the node in the  
211 ecosystem) and *Off* or - (node is absent). We modelled Boolean values through pairs of  
212 complementary places, which is the usual way to work with the absence of test-to-zero in Petri nets  
213 (as a transition cannot test for the absence of a token). For termite ecosystems, an extended graph  
214 made up of 12 nodes was defined as the best compromise between over and under-simplified  
215 descriptions (Table 1).

216 The formal specification of such an ecosystem consists in a triplet  $(\mathbb{E}, s_0, R)$  such that  $\mathbb{E}$  is a set of  
 217 *entities*,  $s_0 \subseteq \mathbb{E}$  is the *initial state*, and  $R$  is a set of *reaction rules* (a process may fire several rules and  
 218 transitions). Entities can be declared with their respective names and initial states (Table 1). The  
 219 initial state  $s_0$  is the set of all the entities declared as initially ‘On’. Here, we chose  $s_0 \stackrel{\text{def}}{=} \{Rp, Sl, At, Ac\}$ ,  
 220 representing reproductives, soil, atmosphere and competitors, respectively. A *state*  
 221 of such a system is defined, like the initial state, by a subset of  $\mathbb{E}$ . For instance, having  $s_0 \stackrel{\text{def}}{=} \{Rp, Sl, At, Ac\}$   
 222 as above means that every entity in  $s_0$  is present (+) in this system state and,  
 223 consequently, every entity in  $\mathbb{E} \setminus s_0$  is absent (-) from this system state.

224 The dynamics of the system is described by a set of *reaction rules* of the form  $(\alpha^+, \alpha^-, \omega^+, \omega^-) \subseteq \mathbb{E}^4$   
 225 such that  $\alpha^+ \cap \alpha^- = \omega^+ \cap \omega^- = \emptyset$ . For convenience, the rules may be numbered and denoted as  
 226  $n: \alpha \rightarrow \omega$  where  $n$  is the identifying number,  $\alpha$  is the list of entities in  $\alpha^+$  followed by a + sign, plus  
 227 the list of entities in  $\alpha^-$  followed by a – sign, and  $\omega$  is similarly defined with  $\omega^+$  and  $\omega^-$ . For example,  
 228 rule 12 in Table 2 is  $(\{Ac\}, \{Sd\}, \emptyset, \{Wk, Rp\})$  and is more conveniently written as 12:  $Ac^+, Sd^- \rightarrow$   
 229  $Wk^-, Rp^-$  as in rewriting systems (Lindenmayer 1978; Gaucherel *et al.* 2012). This rule specifies that  
 230 if  $Ac$  is present and  $Sd$  is absent, then the system may evolve by switching  $Wk$  and  $Rp$  to the  
 231 ‘absent’ state (regardless of their current states, Fig. 3a). For example, translated into ecological  
 232 terms, rule number 12 means that if ant competitors are present when termite soldiers are absent,  
 233 then termite workers and reproductives can be killed (*i.e.* if the rule is applied).

234 A rule  $r \stackrel{\text{def}}{=} (\alpha^+, \alpha^-, \omega^+, \omega^-)$  is *enabled* at a state  $s \in \mathbb{E}$  iff  $(\alpha^+ \subseteq s) \wedge (\alpha^- \cap s = \emptyset)$ ; in such a case,  $r$   
 235 may be *fired*, yielding a new state  $s' \stackrel{\text{def}}{=} (s \setminus \omega^-) \cup \omega^+$ , which is denoted by  $s \xrightarrow{r} s'$ . We ignore firings  
 236 that do not change the state (so-called *self-loops*), for instance, applying Rule 9 when  $Fg$  and  $Sd$  are  
 237 already absent does not bring new information (Table 2). The *state space* of a model is the smallest  
 238 graph  $(E, V)$  such that the initial state is in  $E$  and whenever  $s \in E$  and  $s \xrightarrow{r} s'$  for some rule  $r$ , then  
 239 we also have  $s' \in E$  and there is an edge  $(s, r, s') \in V$ .

## 240 Petri nets semantics of *reaction rules* models

241 By defining the state-space from a set of reaction rules, we have provided its *semantics*, which is the  
242 definition of its behavior. Hence, the reaction rules are just syntactic artefacts; by defining their  
243 semantics, they become the specification of a behavior. Similarly, marking graphs are the semantics  
244 of Petri nets. In this section, we provide another semantics for reaction rules in terms of a translation  
245 to Petri nets. While the state-space semantics is useful to understand systems at a high level of  
246 abstraction, it is not convenient for automated analysis since no tool exists for reaction rules. The  
247 Petri net semantics is a convenient solution to enable the use of the numerous existing theoretical  
248 and software tools to analyze Petri nets. Crucially, at the end of the section, we demonstrate that  
249 both semantics are equivalent (and see Appendix 2), which is a common way of proceeding (Best,  
250 Devillers & Koutny 2001). The Petri net semantics of such systems is computed in two successive  
251 steps. First, (ecological) rules are normalized to make them simpler and unambiguous, then a Petri  
252 net is computed.

## 253 Rule normalization

254 The need for normalization arises from the structure of reaction rules that do not enforce the left-  
255 and right-hand sides of rules to involve exactly the same entities. To illustrate the need for  
256 normalization, consider rule 12:  $Ac^+, Sd^- \rightarrow Wk^-, Rp^-$  given above (Fig. 3a). This rule has two  
257 ambiguities: i) it may be applied regardless of the current state of  $Wk$  and  $Rp$ , which corresponds to  
258 four distinct situations; and ii) it is not complete as it does not specify what happens to  $Ac$  and  $Sd$   
259 after the rule is fired. So, an ecological process may often be considered as a meta-rule in the Petri  
260 net, and the normalization procedure aims at producing unambiguous and complete (exhaustive)  
261 transitions from the meta-rules provided in the specification.

262 For this purpose, we apply two transformations corresponding to the two cases above. Consider a  
263 rule  $r \stackrel{\text{def}}{=} (\alpha^+, \alpha^-, \omega^+, \omega^-)$ , then take  $\alpha \stackrel{\text{def}}{=} \alpha^+ \cup \alpha^-$ ,  $\omega \stackrel{\text{def}}{=} \omega^+ \cup \omega^-$ , and  $\chi \stackrel{\text{def}}{=} \omega \setminus \alpha$ ,  $r$  is replaced by  
264 the set of rules  $R_r \stackrel{\text{def}}{=} \{(\alpha^+ \cup x, \alpha^- \cup (\chi \setminus x), \omega^+, \omega^-) \mid x \in 2^\chi\}$ . Intuitively, the left-hand side of  $r$

265 is augmented in every possible manner so that it becomes a partition of the entities involved in  $r$ ,  
 266 *i.e.*, those from  $\alpha \cup \omega$ . Note that the new rules are still somewhat ambiguous because their left-hand  
 267 side still lacks the entities that are not involved in the original rule, but this will be neatly handled in  
 268 the Petri net semantics. Then, the right-hand sides of the new rules are augmented with the entities  
 269 that appear in  $\alpha$  but not in  $\omega$  so that they are left untouched when the rule is fired, *i.e.* a change that  
 270 is not explicitly specified should not occur, which is consistent with the semantics defined above in  
 271 which  $\alpha$  is not involved in the computation of successor states. So the normalized set of rules  
 272 originated from  $r$  is  $\{(\alpha^+, \alpha^-, \omega^+ \cup (\alpha^+ \setminus \omega), \omega^- \cup (\alpha^- \setminus \omega)) \mid (\alpha^+, \alpha^-, \omega^+, \omega^-) \in R_r\}$ .

273 For example, rule 12:  $Ac^+, Sd^- \rightarrow Wk^-, Rp^-$  is first replaced with the four new rules below by  
 274 completing its left-hand side (Fig. 3b):

- 275 •  $Ac^+, Sd^-, Wk^-, Rp^- \rightarrow Wk^-, Rp^-$
- 276 •  $Ac^+, Sd^-, Wk^-, Rp^+ \rightarrow Wk^-, Rp^-$
- 277 •  $Ac^+, Sd^-, Wk^+, Rp^- \rightarrow Wk^-, Rp^-$
- 278 •  $Ac^+, Sd^-, Wk^+, Rp^+ \rightarrow Wk^-, Rp^-$

279 Then, the right-hand sides of these rules are completed in order to preserve  $Ac$  and  $Sd$ :

- 280 •  $Ac^+, Sd^-, Wk^-, Rp^- \rightarrow Wk^-, Rp^-, Ac^+, Sd^-$
- 281 •  $Ac^+, Sd^-, Wk^-, Rp^+ \rightarrow Wk^-, Rp^-, Ac^+, Sd^-$
- 282 •  $Ac^+, Sd^-, Wk^+, Rp^- \rightarrow Wk^-, Rp^-, Ac^+, Sd^-$
- 283 •  $Ac^+, Sd^-, Wk^+, Rp^+ \rightarrow Wk^-, Rp^-, Ac^+, Sd^-$

284

## 285 Translation into Petri nets

286 The normalized rules can be easily translated into Petri nets in two steps: i) for each entity  $e \in \mathbb{E}$ , two  
 287 places are created:  $e^+$  and  $e^-$  to represent the present and absent states of the entity respectively.  
 288 The rule that corresponds to the initial state given in the specification is marked with one token, the

289 other place is left empty (no token); ii) for each normalized rule in order to preserve  $W_k$  and  $T_e$ :  $r \stackrel{\text{def}}{=} (\alpha^+, \alpha^-, \omega^+, \omega^-)$ , a transition  $t_r$  is added with arcs such that:

- 291 •  $W(e^+, t_r) \stackrel{\text{def}}{=} 1$  for all  $e \in \alpha^+$ ,
- 292 •  $W(e^-, t_r) \stackrel{\text{def}}{=} 1$  for all  $e \in \alpha^-$ ,
- 293 •  $W(t_r, e^+) \stackrel{\text{def}}{=} 1$  for all  $e \in \omega^+$ ,
- 294 •  $W(t_r, e^-) \stackrel{\text{def}}{=} 1$  for all  $e \in \omega^-$ ,
- 295 •  $W(t_r, p) \stackrel{\text{def}}{=} 0$  for any other place  $p$ .

296 The last item above shows how we handle the entities that are not at all involved in a rule.  
297 Moreover, in order to eliminate self-loops here too, we ignore transitions that fire but do not change  
298 the marking (i.e. we do not construct a transition  $t$  whenever  $\vec{\tau} = \vec{t}$ , for instance we shall not  
299 construct the top-most transition in Fig. 3b).

300 At this stage, we demonstrate a theorem that proves a strong equivalence between the reaction  
301 rules and their translation into a Petri net (Appendix 2). In general terms, we prove that the state-  
302 space built from the reaction rules is strongly similar to the marking graph of the Petri net obtained  
303 through the translation of reaction rules into Petri nets (Best, Devillers & Koutny 2001). Both graphs  
304 are isomorphic (i.e. they are identical, yet with labeling that needs to be translated from one graph  
305 to the other). This property is both usual and essential in computer sciences when several layers of  
306 formalism are handled. A precise relationship exists between the two formalisms and their semantics  
307 (Appendix 2, Fig. S1) and the theorem provides a mathematical guarantee that we can study the  
308 marking graph instead of the state-space of the original system.

309 **Theorem 1:** Let  $(\mathbb{E}, s_0, R)$  be a reaction rules model and  $(S, T, W, M)$  be its Petri net semantics. Then,  
310 the state space of  $(\mathbb{E}, s_0, R)$  is isomorphic to the marking graph of  $(S, T, W, M)$  (see the proof in  
311 Appendix 2).

## 312 State space analysis

313 The Petri net of the termite ecosystem is made of 12 ecological components (i.e. nodes, Table 1, Fig.  
314 1b), and 15 ecological processes (i.e. rules, Table 2). The exact Petri net obtained quickly becomes  
315 unreadable (i.e. too many nodes and edges), as the system becomes more complex, but there is no  
316 need to draw it to analyze the system. Rather, as a first analytical step, we can compute its marking  
317 graph (theorem 1). Modelling of the termite colony reaches only 109 states (among  $2^{12}$  possible  
318 states), so that we can draw the exhaustive state-space to visualize it (Fig. 4a). For larger systems, the  
319 analysis can be performed automatically and without drawing the state space too. The state-space  
320 graph obtained here comprises several (colored) elements which we will further describe and  
321 interpret in ecological terms: the initial state (numbered 0, and drawn as a hexagon, Fig. 4a-A), two  
322 topological structures usually called strongly connected components (Fig. 4a-B and 4a-B'), some  
323 decisive paths (e.g. ecosystem trajectories and tipping points, Fig. 4a-C), ultimately leading upward to  
324 some basins and their associated deadlocks (i.e. states from which no other states are reachable, Fig.  
325 4a-D and 4a-D', squares).

326 Any strongly connected component (SCC) is defined as a set of system states (nodes of the state  
327 space) in which every state may be reached from any other state of the SCC. As such, SCCs are  
328 important as they allow the termite ecosystem to run indefinitely, in a kind of dynamic (structural)  
329 equilibrium (see Discussion). From the initial state 0, the system may rapidly evolve to deadlock 2,  
330 always through the execution of rule 12 corresponding to the death of reproductives in the presence  
331 of ant competitors (Fig. 3). Otherwise, the system reaches SCC B (Fig. 4a-B, orange color) when it  
332 fires rules 5, 6, and then 3. So, as a first observation, the system can stay "alive" only if it successively  
333 executes these three rules. If the system stays alive, it reaches the large SCC B. From SCC B, the  
334 system may reach the second large SCC B' (Fig. 4a-B', green). From both SCCs, the system may exit  
335 towards two deadlocks at the left and right hands of the state space, respectively (Fig. 4a-D and 4a-  
336 D'). Deadlocks correspond to states in which the system can no longer evolve, which, in our case,

337 corresponds to ecosystem collapses (i.e. they contain no more termites and cannot recover from any  
338 previous state).

### 339 Strongly connected components

340 The termite system exhibits two large SCCs labeled B and B' (Fig. 4a-B and 4a-B'), within which the  
341 colony may circulate forever. Here, we propose that any SCC is a kind of (qualitative and structural)  
342 stability which behaves like a basin (not to be confused with a "basin of attraction") where it is  
343 possible to stay or occasionally leave. When considered statistically, such SCCs channel the  
344 ecosystem through states which are more numerous for larger basins and take longer to leave for  
345 trajectories further away from the SCC exit. Although the model is qualitative, the number of states  
346 in the SCC and the maximal distance to its exit appear as relevant proxies to quantify the associated  
347 basin.

348 From each state of SCC B where  $Sd$  is present, we can fire rule 11 (soldiers kill ants, Table 2) to reach  
349 a state of SCC B' (but not conversely) that is exactly the same, except that competitors ( $Ac$ ) have  
350 switched to the 'absent' state (both SCCs are isomorphic). This has been checked programmatically  
351 on the state space. However, from every state in SCC B where  $Sd$  is absent, we can fire rule 12 (ants  
352 kill termites) or rule 13 (the absence of fresh air kills termites) and leave the SCC in a deadlock (and  
353 its basin). Considering this isomorphism, we can concentrate on SCC B' only, and zoom in on it by  
354 hiding states outside the SCC (Fig. S3a). The higher the distance to exit (in steps) the SCC, the less  
355 likely the system leaves the SCC and reaches another basin containing a deadlock leading to the  
356 inevitable (structural) collapse of the system. A state labeled with a null exit distance does not  
357 necessarily mean that the system *will* exit, rather that it *may* exit into a single move. By more finely  
358 studying the SCC B' graph, it is possible to list many other observations on the termite system  
359 behavior (see Appendix 3 and Fig. S3 for a refined analysis).

## 360 System trajectory, tipping points and collapses

361 To focus on system trajectory instead of system states, it is possible to compute the marking graph in  
362 which SCCs have been reduced to a single node (also called the SCC graph or merged state space, Fig.  
363 4b). When not reduced, this trajectory graph may rapidly become unreadable. It is possible to  
364 automatically (via programming) simplify this SCC graph by merging basins to a single node including  
365 the deadlock they lead to (Fig. 4b). From this convenient reduction of the ecosystem trajectories, it  
366 becomes easy to identify specific and contrasting paths leading to the ecosystem collapse (Fig. 4b,  
367 squares), and the tipping points separating them (e.g. Fig. 4a, red segment, see Appendix 3 for a  
368 refined analysis of trajectories).

369

## 370 Discussion

371 A goal of ecology is to develop strategies and tools for mapping an ecosystem's long-term dynamics,  
372 as well as some dynamical properties such as basins and sharp transitions (e.g. tipping points, TPs).  
373 This issue is a real challenge and with current models it can be hard to quantify the resilience and  
374 changes associated with such properties (Walker *et al.* 2004; Scheffer *et al.* 2015). For this purpose,  
375 we have defined and illustrated—for the first time to our knowledge—a powerful model class to  
376 formalize ecosystem behaviors. No restriction on types of ecological components (biotic, abiotic or  
377 anthropic) and interactions (e.g. ecological or socio-economical) are imposed by such integrated  
378 models. Petri nets, already widely used in biology and in social sciences (Murata 1989; Blätke, Heiner  
379 & Marwan 2011; Koch, Reisig & Schreiber 2011) along with other qualitative models (Kauffman 1969;  
380 Thomas & Kaufman 2001), have demonstrated here their ability to model a theoretical complex  
381 ecosystem.

382 The Petri net model developed here rigorously and successfully computed every possible state and  
383 trajectory encountered by the termite ecosystem (Fig. 4a). The model also automatically computed

384 qualitatively stable (resilient, SCC) and unstable (tipping point) zones (Fig. 4b). Although qualitative,  
385 such models can compute many quantitative metrics from the large state space provided.

386

### 387 [Understanding the termite ecosystem](#)

388 The termite colony was represented as a relational network between biotic and abiotic components  
389 that was allowed to initiate, grow and die, depending on ecological rules and disturbances applied to  
390 the network (Fig. 4). We stress the conceptual difference between system *functioning*, focusing on  
391 the (often short term) abundance and flux variations between system components, whilst keeping  
392 the system structure unchanged, and system *development*, focusing on the (often long term,  
393 topological) system structure changes (Odum & Odum 1971; Gaucherel *et al.* 2017). While this  
394 qualitative model allows the modeling of a large and complex interaction network, it identifies only  
395 *possible* fates, without their occurrence probabilities. As a perspective, a quantitative Petri net model  
396 would also provide the confidence interval for frequent (highly probable) and unrealistic (highly  
397 improbable) trajectories.

398 As soon as the ecosystem model is built and its simplifications assumed, the state space of the  
399 modeled ecosystem is automatically computed and reveals insights into the ecosystem dynamics  
400 (called the *development*, Fig. 4). Starting with the system growth from an initial state composed only  
401 of reproductives (and the permanent soil and atmosphere environment), two kinds of colony  
402 collapse can occur. Collapse of the termite colony, i.e. states in which the system is paralyzed, are  
403 always reached after reproductive death, due to the lack of breathing air in the nest (rule 13) or an  
404 attack by ant competitors (rule 12) (Turner 2009). Reproductives are the sole component in the  
405 model that are able to produce workers and egg chambers (rules 4 and 2). Hence, our model allows  
406 for the rigorous detection of decisive rules, i.e. tipping points with irreversible effects, that inevitably  
407 lead to system collapse (Costa & Fitzgerald 2005; Turner 2009). Conversely, if reproductives remain  
408 alive, the system may remain indefinitely in similar states by first producing workers and

409 termitomyces (mushrooms), and then by traveling through many trajectories of creation/destruction  
410 cycles. The “resilient” states (SCCs B and B’) act as structural basins of attraction and remain  
411 unchanged as long as no ant competitors arrive in the system. Such non-trivial global features (see  
412 Appendix 3 for other added values) would not have been detected without the use of this model  
413 exploring exhaustively the system behavior.

414 These results confirm the central roles of the reproductives and air quality of the nest, as well as the  
415 minor roles of workers, soldiers and other components that the termite system can rapidly  
416 regenerate, as found in real colonies (Costa & Fitzgerald 2005; Turner 2009). The result also  
417 highlights the importance of modeling assumptions. For example, adding a new rule allowing the  
418 workers to regenerate reproductives would have drastically changed the ecosystem fates, while  
419 many other rules would not have changed the state space at all. Adding such a decisive rule mimics  
420 ecological engineering practices designed to restore a disturbed ecosystem (DeAngelis *et al.* 1998;  
421 Pfadenhauer 2001). From another perspective, our discrete model could also be used to qualitatively  
422 study the system’s sensitivity to additional rules (ecological processes) and the way such rules may  
423 degrade or improve the ecosystem’s resilience (rules 2 and 4, or 7, Fig. 5). The sensitivity of discrete  
424 models to changes in the rules driving the behavior has also been studied in the context of Boolean  
425 networks applied to the modelling of biological systems (Saadatpour *et al.* 2011; Gaucherel *et al.*  
426 2017).

#### 427 [Discrete and qualitative ecosystem models](#)

428 The main originality of our work not only lies in the use of discrete models (e.g. Petri nets) in ecology,  
429 as some other studies started to explore the promising avenue of discrete models too (Ewing *et al.*  
430 2002; Gaucherel *et al.* 2012; Baldan *et al.* 2015; Gaucherel *et al.* 2017). Rather, it concerns the  
431 discrete and qualitative conception of the integrated ecosystem forming, we think, the backbone of  
432 any ecosystem. The discrete engine behind our model then allows an exhaustive and rigorous  
433 exploration of the ecosystem behaviour. This observation is striking considering that almost all

434 ecosystem or species community models focus on more continuous and gradual changes (Thébault &  
435 Fontaine 2010; Kéfi *et al.* 2016).

436 The formal modeling of dynamic ecological systems has traditionally been carried out using  
437 differential equations (Thébault & Fontaine 2010; Kéfi *et al.* 2016). However, discrete modelling  
438 developed in computer sciences has proven to be successful, in particular in systems biology  
439 (Lindenmayer 1978; Campbell *et al.* 2011; Gaucherel *et al.* 2012). The two approaches can be  
440 considered as complementary: while traditional differential equations usually provide quantitative  
441 *mean field* behavior for the system, discrete modelling enables a qualitative analysis of *every*  
442 behavior. This is notably done through the inventory of the system states, of some system  
443 characteristic events, through the decomposition of the system trajectories, of causality, and of  
444 independence (Pommereau 2010; Koch, Reisig & Schreiber 2011). Discrete models often capture the  
445 trajectories of the dynamic system more accurately (Cordier, Largouët & Zhao 2014; Gaucherel *et al.*  
446 2017). For example, in the termite colony we modeled, differential equations would have certainly  
447 identified the pivotal role of rules 12 and 13 in the system collapse (Fig. 4a-C), but it would have been  
448 difficult to confirm that these rules are the only ones that are dangerous for the colony. For the same  
449 reason, differential equations would not have easily identified and characterized the termite colony-  
450 specific scenarios on both sides of the tipping point. While some property identifications here could  
451 have been perceived *a posteriori* as trivial, Petri nets show the same power for identifying any  
452 (potentially complex) basins and tipping points.

453 Our formal model defined two semantics that we showed were equivalent. The first semantics is  
454 called *operational*, because it defines states and provides the operations to execute one transition  
455 (rule) to reach another state. The second semantics is called *denotational* because it transforms  
456 states and rules into new objects, i.e., Petri nets that are associated with their own semantics.  
457 Operational semantics is useful to describe ecological aims with formal modeling as directly as  
458 possible: it rigorously grasps the notions needed to understand the ecosystem at the adequate level

459 of abstraction (Koch, Reisig & Schreiber 2011). However, semantics is a mathematical definition only,  
460 and no software tool exists to handle it. These tools may be developed, but it is more straightforward  
461 to define an equivalent denotational semantics and the tool required for the translation only.

462 To define the denotational semantics of this study, we chose a Petri net translation well adapted to  
463 network handling, although other formalisms exist (Lindenmayer 1978; Thomas & Kaufman 2001;  
464 Gaucherel *et al.* 2012; Giavitto, Kludel & Pommereau 2012). Petri nets are widely acknowledged as  
465 a useful modelling formalism for building discrete models of biological systems. Among their  
466 benefits, the following are often emphasized (Machado *et al.* 2009): simplicity, as Petri nets are easy  
467 to understand and adopt for biological situations, while still allowing a large flexibility (called  
468 expressivity); graphical representation that both conveys intuition and allow topological analysis;  
469 modularity that allows the building of large models by assembling smaller blocks and the potential to  
470 be extended in many different ways (see below).

#### 471 [On the benefits of Petri nets](#)

472 We note three key benefits of using Petri nets: the adequacy to express the denotational semantics  
473 of our nodes/rules-based formalism, the wide range of analyzing techniques and available tools, and  
474 the flexibility that opens the way to future extensions. For example, it is straightforward to add  
475 features like priorities, time, stochasticity and quantitative data (David & Alla 2010). Any Petri net  
476 may become quantitative by adding a number of tokens in various places (multivalued nets,  
477 Pommereau 2010; Reisig 2013). This flexibility allows us to foresee in ecology many possible  
478 extensions of the current setting. Yet, the 'reachability graph' of Petri nets suffers from the well-  
479 known 'state explosion' problem, that is, the reachability graph may be exponentially larger than the  
480 corresponding Petri net. This observation limits the size of the models providing an explicit  
481 computation of their reachability graphs, although we already manage large graphs composed of  
482 more than four million states. However, symbolic techniques exist, such as decision diagrams  
483 (Hamez, Thierry-Mieg & Kordon 2008), to alleviate the explosion of the state space.

484 When considering extensions to Petri nets, a wide range of methods and software tools are available  
485 to develop and analyze them (Haustermann *et al.* 2017). Here, we used a custom marking graph  
486 analysis, with the aggregation of strongly connected components and the basins (Fig. 4). We used the  
487 SNAKES toolkit (Pommereau 2015) to implement the denotational semantics, the TINA toolkit to  
488 compute the marking graph (Berthomieu 2017), and custom tools to perform the analyzing steps. In  
489 the future, we plan to extend the structural analysis available with Petri nets and in particular to  
490 exploit its transitions- and places-invariants, or traps.

491 To adapt Petri nets for an ecological system, we first designed a modelling language (reaction rules)  
492 intended to be directly used by ecologists and to explicitly define the concepts dealt with, e.g.,  
493 ecological components, and elementary processes. This formalism has to be self-contained and to  
494 include operational semantics, including diagnostics, to allow the modeler a high-level of abstraction.  
495 In addition, we need a denotational semantics to access existing analyses and software tools. Petri  
496 nets are suitable for translating the high-level formalism, as nodes and rules naturally map onto  
497 places and transitions, respectively. Other methods such as automata or process algebra are also well  
498 suited to define parallel processes, but communication is usually handled through transition  
499 synchronization, whereas ecologists need resource sharing with concurrent accesses. Boolean  
500 networks are well suited for modelling ecological nodes (Gaucherel *et al.* 2017), but they handle  
501 deterministic processes only and are not as open to extensions as in Petri nets. Petri nets are  
502 probably the most versatile discrete modeling framework in life sciences (Machado *et al.* 2009),  
503 which explains their recent popularity growth in systems biology.

#### 504 [Ecosystem resilience and tipping points](#)

505 The Petri net model is powerful in describing ecosystem development, and other ecosystem-related  
506 concepts. SCCs and associated basins play the role of relatively stable zones (Walker *et al.* 2004;  
507 Scheffer *et al.* 2015; Karssenberg, Bierkens & Rietkerk 2017), as the termite ecosystem may run  
508 indefinitely into such structures. Such resilient states of the ecosystem, automatically identified by

509 the Petri net analysis, are reminiscent of phenotypes of a living organism in biology (Blätke, Heiner &  
510 Marwan 2011; Koch, Reisig & Schreiber 2011). Phenotypes can be likened to basins keeping the  
511 system in a specific set of states although, in our model, such zones locally “attract” the system only  
512 when it enters these SCCs. It is possible to quantify the width of the basin by the number of states it  
513 contains (or by any other related variable) (e.g. 20 states in SCC B', Fig. 4 and Fig. S3). It is also  
514 possible to quantify the precariousness of the system at any state by the distance to exit the SCC,  
515 while the maximal distance to exit may naturally quantify the maximal system resilience in this basin  
516 (e.g., a depth of 3 in SCC B', Fig. S3). In addition, any shift between distinct SCCs or between any SCC  
517 and a basin containing a deadlock corresponds precisely to tipping points (Hirota *et al.* 2011; van Nes  
518 *et al.* 2014). The state-space provides a rigorous way to exhaustively identify these ecological  
519 features and other, e.g. specific trajectories, for any ecosystem, theoretically and as long as the  
520 system has been accurately understood and modeled.

521 So far, we have justified the qualitative conception of ecosystems by long term dynamics under  
522 study. However, our model is not dedicated to any spatial or temporal scale or to closed ecosystems,  
523 as matter and energy inputs (e.g. due to global changes or to evolution, Weber *et al.* 2017) may be  
524 integrated as additional nodes. The qualitative assumption rather assumes that the ecosystem graph  
525 forms the backbone of the system and provides deep insight into its overall behaviour (called the  
526 ecosystem development, Gaucherel *et al.* 2017). In the future, we aim to apply Petri nets to more  
527 complex spatial and temporal scales, ranging from a small pond over days to a continent over million  
528 years, with coherent management of each scale. In addition to methodological advantages previously  
529 mentioned, the advantages we see for all these ecological applications of discrete and qualitative  
530 models are the abilities: i) to integrate components of distinct natures, ii) to easily handle changing  
531 topologies of the ecological interactions involved, iii) to formalize the model and rigorously  
532 demonstrate its outputs, and iv) to capture the causality of the system dynamics (in the state space).

533

534 In conclusion, we suggest that Petri nets provide a new class of models for analyzing ecosystem  
535 behaviors and formalizing ecosystem development over the long term. The development concept is  
536 fully coherent with drastic regime shifts and with resilience in ecosystem dynamics, and Petri nets  
537 are a powerful and rigorous class of discrete models able to identify, handle and quantify ecosystem-  
538 related concepts. In our conceptual view, any ecosystem may be modelled in an integrated way and  
539 such a model provides the exhaustive trajectories based on the model assumptions. Using Petri nets  
540 supposes that every ecosystem can be represented on the basis of its relational graph (interaction  
541 network) connecting every relevant component of the ecosystem through any relevant process. The  
542 ecosystem graph is then rigorously handled with a discrete model exhaustively modifying graph  
543 topology, which is the real added value of our model. To our knowledge, this approach has not yet  
544 been used in an example of an ecological situation. The existence of a wide range of disturbed  
545 ecological networks opens an avenue to this new way of identifying resilience and tipping points over  
546 the long term.

547

548

## 549 References

- 550 Baldan, P., Bocci, M., Brigolin, D., Cocco, N. & Simeoni, M. (2015) Petri nets for modelling and  
551 analysing trophic networks. *BioPPN 2015, a satellite event of PETRI NETS 2015* (eds M. Heiner  
552 & A.K. Wagler). CEUR Workshop Proceedings.
- 553 Berthomieu, B. (2017) The TINA toolkit. <http://projects.laas.fr/tina//home.php>.
- 554 Best, E., Devillers, R. & Koutny, M. (2001) *Petri Net Algebra*. Springer, Berlin.
- 555 Blätke, M.A., Heiner, M. & Marwan, W. (2011) *Tutorial. Petri Nets in Systems Biology*. Otto-von-  
556 Guericke University Magdeburg, Germany.
- 557 Campbell, C., Yang, S., Albert, R. & Sheab, K. (2011) A network model for plant-pollinator community  
558 assembly. *proceedings of the National Academy of Sciences (PNAS)*, **108**, 197-202.
- 559 Carpenter, S.R. (2003) *Regime shifts in lake ecosystems*. Ecology Institute, Oldendorf/Luhe, Germany.
- 560 Cordier, M.-O., Largouët, C. & Zhao, Y. (2014) Model-Checking an Ecosystem Model fo Decision-Aid.  
561 *IEEE 26th International Conference on Tools with Artificioal Intelligence*, pp. 539-543. IEEE  
562 Computer Society.
- 563 Costa, J.T. & Fitzgerald, T.D. (2005) Social terminology revisited: Where are we ten years later? *Ann.*  
564 *Zool. Fennici*, **42**, 559-564.
- 565 David, R. & Alla, H. (2010) *Discrete, Continuous, and Hybrid Petri Nets*. Springer, Berlin, Heildelberg,  
566 Germany.
- 567 DeAngelis, D.L. (1980) Energy-flow, nutrient cycling, and ecosystem resilience. *Ecology*, **61**, 764–771.
- 568 DeAngelis, D.L., Gross, L.J., Huston, M.A., Wolff, W.F., Fleming, D.M., Comiskey, E.J. & Sylvester, S.M.  
569 (1998) Landscape modeling for everglades ecosystem restoration. *Ecosystems*, **1**, 64-75.
- 570 Ewing, B., Yandell, B., Barbieri, J., Luck, R. & Forster, L. (2002) Event-driven competing risks.  
571 *Ecological Modelling*, **158**, 35-50.
- 572 Fowler, H.G., Pereira da-Silva, V., Forti, L.C. & Saes, N.B. (1986) Population dynamics of leaf cutting  
573 ants: A brief review. *Fire ants and leaf-cutting ants*, pp. 123–145. Westview Press, Colorado,  
574 Boulder.

575 Gaucherel, C. (2010) Self-organization of patchy landscapes: Hidden optimization of ecological  
576 processes. *Journal of Ecosystem & Ecography*, **1**.

577 Gaucherel, C., Boudon, F., Houet, T., Castets, M. & Godin, C. (2012) Understanding Patchy Landscape  
578 Dynamics: Towards a Landscape Language. *PLoS ONE*, **7**, e46064.

579 Gaucherel, C., Théro, H., Puiseux, A. & Bonhomme, V. (2017) Understand ecosystem regime shifts by  
580 modelling ecosystem development using Boolean networks. *Ecological Complexity*, **31**, 104-  
581 114.

582 Giavitto, J.-L., Kludel, H. & Pommereau, F. (2012) Integrated regulatory networks (IRNs): Spatially  
583 organized biochemical modules. *Theoretical Computer Science*, **431** 219-234.

584 Hamez, A., Thierry-Mieg, Y. & Kordon, F. (2008) Building efficient Model-Checkers using hierarchical  
585 Set Decision Diagrams and Automatic Saturation. *Fundamenta Informatica Petri Nets (IOS*  
586 *Press)*, 1-25.

587 Haustermann, M., Wagner, T., Moldt, D., Heitmann, F., Rölke, H., Mortensen, K.H., Kummer, O. &  
588 Christensen, S. (2017) Petri Nets Tool Database. Petri Nets World.

589 Hély, C., Braconnot, P., Watrin, J. & Zheng, W. (2009) Climate and vegetation : Simulating the African  
590 Humid Period. *Comptes Rendus Géoscience*, **341**, 671-688.

591 Hély, C., Shuggart, H.H., Swap, B. & Gaucherel, C. (2019) The Drape Concept to Understand  
592 Ecosystem Dynamics and its Tipping Points. *Submitted*.

593 Hirota, M., Holmgren, M., Van Nes, E.H. & Scheffer, M. (2011) Global Resilience of Tropical Forest  
594 and Savanna to Critical Transitions. *Science*, **334**, 232-235.

595 Holling, C.S. (1973) Resilience and stability of ecological systems. *Annu. Rev. Ecol. Syst.*, **4**, 1-23.

596 Karssenber, D., Bierkens, M.F.P. & Rietkerk, M. (2017) Catastrophic Shifts in Semiarid Vegetation-  
597 Soil Systems May Unfold Rapidly or Slowly. *American Naturalist*, **190**, E145–E155.

598 Kauffman, S.A. (1969) Metabolic stability and epigenesis in randomly constructed genetic nets.  
599 *Journal of theoretical biology*, **22**, 437-467.

600 Kéfi, S., Miele, V., Wieters, E., Navarrete, S. & Berlow, E. (2016) How Structured Is the Entangled  
601 Bank? The Surprisingly Simple Organization of Multiplex Ecological Networks Leads to  
602 Increased Persistence and Resilience. *PLoS Biology*, **14**, e1002527.

603 Koch, I., Reisig, W. & Schreiber, F. (2011) *Modeling in systems biology. The Petri net approach*.  
604 Springer-Verlag, London, UK.

605 Lenton, T.M., Livina, V.N., Dakos, V. & Scheffer, M. (2012) Climate bifurcation during the last  
606 deglaciation? *Climate of the Past*, **8**, 1127-1139.

607 Lindenmayer, A. (1978) Algorithms for plant morphogenesis. *Theoretical plant morphology* (ed. R.  
608 Sattler), pp. 37-81. Leiden University Press, The Hague.

609 Machado, D., Costa, R.S., Rocha, M., Rocha, I., Tidor, B. & Ferreira, E.C. (2009) A Critical Review on  
610 Modelling Formalisms and Simulation Tools in Computational Biosystems. *International*  
611 *Work-Conference on Artificial Neural Networks* (ed. A.I. IWANN : Distributed Computing,  
612 Bioinformatics, Soft Computing, and Ambient Assisted Living), pp. 1063-1070. Part of the  
613 Lecture Notes in Computer Science book series (LNCS).

614 Murata, T. (1989) Petri nets: Properties, analysis and applications. *Proceedings IEEE*, **77**, 541-580.

615 Odum, E.P. & Odum, H.T. (1971) *Fundamentals of ecology*, 3rd edn. Saunders, Philadelphia, US.

616 Pfadenhauer, J. (2001) Some remarks on the socio-cultural background of restoration ecology.  
617 *Restoration Ecology*, **9**, 220-229.

618 Pommereau, F. (2010) Algebras of coloured Petri nets. *Lambert Academic Publishing (LAP)*.

619 Pommereau, F. (2015) SNAKES. A flexible high-level Petri nets library. *Proceedings of PETRI NETS'15*.  
620 LNCS 9115. Springer

621 Reisig, W. (2013) *Understanding Petri Nets*. Springer Berlin Heidelberg, Berlin, Heidelberg.

622 Saadatpour, A., Wang, R.-S., Liao, A., Liu, X., Loughran, T., Albert, I. & Albert, R. (2011) Dynamical and  
623 Structural Analysis of a T Cell Survival Network Identifies Novel Candidate Therapeutic  
624 Targets for Large Granular Lymphocyte Leukemia. *PLoS Comput Biol*, **7**, e1002267.

625 Scheffer, M. (2009) *Critical Transitions in Nature and Society*. Princeton Univ. Press, Princeton, NJ.

626 Scheffer, M., Carpenter, S., Foley, J.A., Folke, C. & Walker, B. (2001) Catastrophic shifts in ecosystems.  
627 *Nature*, **413**, 591-596.

628 Scheffer, M., Carpenter, S.R., Dakos, V. & van Nes, E.H. (2015) Generic Indicators of Ecological  
629 Resilience: Inferring the Chance of a Critical Transition. *The Annual Review of Ecology,*  
630 *Evolution, and Systematics*, **46**, 145-167.

631 Scheffer, M., Hosper, S.H., Meijer, M.L., Moss, B. & Jeppesen, E. (1993) Alternative equilibria in  
632 shallow lakes. *TRENDS in Ecology and Evolution*, **8**, 275-279.

633 Thébault, E. & Fontaine, C. (2010) Stability of Ecological Communities and the Architecture of  
634 Mutualistic and Trophic Networks. *Science*, **329**, 853 -856.

635 Thom, R. (1975) *Structural stability and morphogenesis*. Benjamin, Reading, MA.

636 Thomas, R. & Kaufman, M. (2001) Multistationarity, the basis of cell differentiation and memory. II.  
637 Logical analysis of regulatory networks in terms of feedback circuits. *Chaos*, **11**, 180-195.

638 Turner, J.S. (2009) *The extended organism: the physiology of animal-built structures*. Harvard  
639 University Press.

640 van Nes, E.H., Hirota, M., Holmgren, M. & Scheffer, M. (2014) Tipping points in tropical tree cover:  
641 linking theory to data. *Global Change Biology*, **20**, 1016-1021.

642 Van Nes, E.H. & Scheffer, M. (2007) Slow Recovery from Perturbations as a Generic Indicator of a  
643 Nearby Catastrophic Shift. *American Naturalist*, **169**, 738-747.

644 Walker, B., Holling, C.S., Carpenter, S.R. & Kinzig, A. (2004) Resilience, adaptability and  
645 transformability in social-ecological systems. *Ecology and Society*, **9**, 5.

646 Weber, M.G., Wagner, C.E., Best, R.J., Harmon, L.J. & B. Matthews (2017) Evolution in a Community  
647 Context: On Integrating Ecological Interactions and Macroevolution. *Trends in Ecology &*  
648 *Evolution*, **32**, XXX.

649

650

## 651 Author contribution statement

652 Author contributions: C.G. and F.P. conceived the ideas and the model, analysed its outputs and led  
653 the writing together.

654

## 655 Acknowledgments

656 We thank Cinzia Di Giusto for discussions on ecosystem definition and Serguei Verlan for discrete  
657 model specificities.

658

## 659 Data Accessibility

660 Readers interested may find the PNML file at this URL <https://zenodo.org/record/3241370> (DOI :  
661 10.5281/zenodo.3241370).

662

## 663 SUPPLEMENTARY MATERIAL - APPENDICES

664 [Appendix 1: The functioning of termite and ant colonies](#)

665 [Appendix 2: Proof of theorem 1](#)

666 [Appendix 3: State-space refined analysis](#)

667

## 668 Tables

669

670 Table 1. Node categories, names, abbreviations, and descriptions of the extended termite ecosystem  
 671 graph (see Fig. 1a for their interactions and associated colors).

672

<i>Name</i>	<i>initially</i>	<i>family</i>	<i>description</i>	<i>comment</i>
<i>Rp</i>	present	inhabitants	reproductives	the queen, the king, the eggs and the nymphs
<i>Wk</i>	absent	inhabitants	workers	all termites able to work: the larvae, workers, pseudo-workers
<i>Sd</i>	absent	inhabitants	soldiers	the termite soldiers
<i>Te</i>	absent	inhabitants	termitomyces	the fungus cultivated by the termites
<i>Ec</i>	absent	structures	egg chambers	all egg chambers plus the royal chamber
<i>Fg</i>	absent	structures	fungal gardens	all the gardens in which the fungus is grown
<i>Md</i>	absent	structures	mound	the upper structure of the colony
<i>Wd</i>	absent	resources	wood	the wood stored inside the colony
<i>Ai</i>	absent	resources	air of the nest	the air inside the colony
<i>Sl</i>	present	environment	soil	the soil around the termite nest
<i>At</i>	present	environment	atmosphere	the air around the termite nest
<i>Ac</i>	present	competitors	ant competitors	all the ant species in competition with the termites

673

674

675 Table 2. List of the rules modeling the termite ecosystem functioning and development. The order of  
676 priority (sequence), the conditions of application, the products (consequences), and a detailed  
677 explanation are given for each rule. The rule arrows indicate the transformation (rewriting) of the  
678 network at next step.  
679

<i>Rule</i>	<i>comment</i>
1: $Wk^+, Te^+ \rightarrow Wd^-, Ai^-$	the workers and the fungi are consuming wood and air
2: $Fg^- \rightarrow Te^-$	the fungi need the fungal gardens in order to survive
3: $Wk^+, Sl^+ \rightarrow Wd^+, Te^+, Fg^+, Ec^+, Md^+$	the workers are foraging in the soil for wood and fungus; from the soil, the workers are building the fungal gardens, the egg chambers, and the mound
4: $Wd^- \rightarrow Wk^-, Te^-$	the workers and the fungus need to eat wood to survive
5: $Rp^+, Sl^+ \rightarrow Ec^+$	for the soil, the queen and the king can also build egg rooms
6: $Rp^+, Ec^+ \rightarrow Wk^+$	in the egg chambers, the queen and the king are producing eggs that are becoming workers
7: $Wk^+, Wd^+ \rightarrow Sd^+, Rp^+$	eating some wood, the larvae are metamorphosing into soldiers and/or nymphaea
8: $Md^+, At^+ \rightarrow Ai^+$	the air of the nest is being refreshed by passing through the mound and exchanging with the atmosphere

9: $Wk^- \rightarrow Fg^-, Sd^-$	the soldiers cannot survive without the workers to feed them, and the fungal gardens need some maintenance by the workers
10: $Wk^-, Rp^- \rightarrow Ec^-$	the egg chambers need some maintenance by the workers or the reproductives, otherwise they collapse
11: $Sd^+ \rightarrow Ac^-$	the soldiers are killing ant competitors intruding into the colony
12: $Ac^+, Sd^- \rightarrow Wk^-, Rp^-$	without the soldiers, the ant competitors are invading the colony and killing the workers and the reproductives
13: $Ai^- \rightarrow Rp^-, Wk^-, Te^-$	the reproductives, the workers and the fungus need to breath the air of the nest to survive

680

681

## 682 Figures

683

684 Figure 1. Graphic of a termite colony (a) and its simplified interaction network (b). Termites modify  
685 their environment and build a mound with various chambers to host the colony (a). The original  
686 ecosystem graph is composed of 12 nodes (Table 1) with five colors representing their different  
687 natures (b, left). Their 15 respective interactions (processes, Table 2) are oriented (b, edges are  
688 directed from the thin to the thick end).

689

690 Figure 2. Illustration of a simplistic predator-prey system (a), with its qualitative dynamics (b), its  
691 associated Petri net (c) and marking graph (d). The system is made of two ecosystem components,  
692 the prey (N) and predator (P) populations, and two interactions connecting them (rules R1 and R2),  
693 as seen on the automaton (a). Starting with the presence of both populations, it is possible to list all  
694 system states encountered (b), and to connect them with the rules (absent components and  
695 inactivated rules are displayed in grey). The corresponding Petri net is made of four places (P+, P-,  
696 N+, N-) and two transitions R1 and R2, where unlabeled arcs have weight 1. The net is depicted in the  
697 initial state (c), and the successive states may be deduced from the token circulation seen in the  
698 dynamics (b). The marking graph of the Petri net (d) is depicted with each state number ( $S_0, S_1, S_2$ )  
699 referring to the dynamics described above (b). Notice that the (sole) specific state of the system ( $S_3$ )  
700 may not be reached from this initial condition and with these rules (d).

701

702 Figure 3. Focus on the rule 12 (Table 2) of the termite ecosystem modeled, based on the extended  
703 graph (a) and translation of the rule (b). Starting from the complete ecosystem (a, left), the rule  
704 12:  $Ac^+, Sd^- \rightarrow Wk^-, Rp^-$  is drawn by the use of involved nodes only (a, right), where conditional  
705 nodes are shown in green and final nodes in gray. However, this diagram is not rigorous enough in

706 that it does not make explicit how to proceed to apply the rule (see main text). The rule is therefore  
707 normalized into four distinct transitions (b). Each transition  $t_i$  corresponds to a distinct normalized  
708 rule. In bold, the rule indeed fired.

709

710 Figure 4. The full (a) and reduced (b) marking graph of the Petri net provides the semantics of the  
711 termite model. The state-space is made of 109 states labeled with a pair  $n/s$  where  $n$  is an  
712 identifying number of the marking and  $s$  is the number of the strongly connected states (SCC) and of  
713 the basin it belongs to. The initial state is displayed as a hexagon (A), deadlocks (states with no  
714 successors) are displayed as squares (five in total, among which two are in zones D and D', and one is  
715 close to the initial state A), a tipping point is displayed as a red segment (C) and other states are  
716 displayed as circles. Each SCC or basin uses a distinct color (e.g. SCCs B and B' are drawn in orange  
717 and green). The edges are directed from the thin to the thick end and labeled with the number of the  
718 rule that was applied to perform the transition. The rule numbers are those of the ecological model  
719 (Table 2) and do not refer to the normalized rules (that are necessary technical steps, but do not  
720 make sense to the modeler). In the simplified and more abstract versions of the marking graph of a  
721 termite model (b), each SCC and basin has been reduced to a single node and redundant paths have  
722 been removed. Nodes representing aggregate SCCs or basins are noted ( $s$ ) (circles), more easily  
723 highlighting the sharp transitions between them. From this reduction of the marking graph, specific  
724 paths leading to the main ecosystem collapses can be more easily identified (squares).

725

1  
2  
3  
4  
5  
6  
7  
8  
9  
10  
11

**Using discrete systems to  
exhaustively characterize the  
dynamics of an integrated ecosystem**

*SUPPLEMENTARY MATERIAL - APPENDICES*

## 12 Appendix 1: The functioning of termite colony

13

14 Macrotermitinae, also called fungus-growing termites, are an African and SE Asian sub-  
15 family of Termitidae (Engel & Krishna 2004). The only known lineage of termites living in  
16 symbiosis with fungi, they are well known for the huge mounds they build. In the early  
17 stages of a (monogamous) colony, the (single) queen and king pair up during the nuptial  
18 flight (Shellman-Reeve 1990; Rosengaus & Traniello 1991; Shellman-Reeve 1997), and then  
19 build a room in the soil. They lay eggs that develop into larvae. Larva development follows  
20 various pathways, the individuals becoming either workers or soldiers (the sterile line), or  
21 nymphaea that later develop into alates (the reproductive line) (Noirot 1955). Alates fly  
22 away during the next nuptial flight or, if needed, they can replace the royal pair or even  
23 transform into pseudo-workers (Noirot 1956). Termites experience hemimetabolous  
24 development, as immature stages have miniature adult morphology, and are therefore fit  
25 for labor.

26 Macrotermitinae live in a nest separated from their source of food (wood), so that workers  
27 have to forage outside the nest. During the first forage, the workers harvest the  
28 basidiospores of the *Termitomyces* species fungus (e.g. (Noirot 1955)) and grow them in  
29 gardens. Termites can digest the wood with the help of the preliminary fungus-performed  
30 lignin degradation process (Hyodo *et al.* 2000). The workers are also in charge of nest  
31 building, fungus care, and egg care. Soldiers protect the colonies and alates that are inactive.  
32 A mature termite nest contains a royal chamber, egg rooms, and fungus gardens below the  
33 surface and a mound above the surface, in order to regulate the composition and  
34 temperature of the air (Turner 2009). Many other species live inside their nest: fungus  
35 species of the *Xylaria* genus, the main parasites in the fungus garden, and other commensal  
36 species (Jaffe, Ramos & Issa 1995), while ants, the primary predator of termites, can invade  
37 their colony (Leal & Oliveira 1995).

38

39 To simulate the foundation of a termite colony (i.e. initial state), only the Soil, Atmosphere,  
40 Reproductives and Air nodes of the nest were set to On, the other nodes being absent (Off).  
41 Although Off nodes are present in the graph for modeling ease, they allow to mimic, by their  
42 very absence, a graph growth (i.e. development) coherent with other approaches in discrete  
43 modeling (Godin 2000; Giavitto & Michel 2003; Sayama & Laramée 2009). So, the Petri net  
44 developed here could later be improved into more complicated models. In order to capture  
45 the colony's dynamics, we then defined a finite set of rules establishing how node states  
46 changed over time. A transition (rule) is an oriented relationship between the states of  
47 nodes at time step  $t$  and the states of the same or other nodes at time step  $t+1$ , according to  
48 certain conditions. In the case of the termite ecosystem and qualitative Petri net, transitions  
49 are simple, a state of "if then" (i.e. Boolean) rules (Thomas & Kaufman 2001; Giavitto &  
50 Michel 2003). All the (potentially applicable) rules were applied at each time step, checking  
51 their associated conditions and whether they changed the state of the system or not (Tables  
52 2), independently of the updated state of each node (i.e. each state was memorized and  
53 then taken as the initial state for all rule applications of the next step).

54

55 Even when absent, the nodes pre-exist (i.e. the graph is fixed), thus highlighting the main  
 56 difference with more complex graph-grammar models. For example, in the termite colony,  
 57 the Wood node was Off at the beginning of the simulation, because this resource had not  
 58 yet been introduced to the colony. This ecological process also meant that workers and  
 59 wood nodes were connected by an oriented edge in the ecosystem's graph (Fig. 1a). For  
 60 termite and ant ecosystems, extended graphs made up of 13 nodes were defined (Tables 1  
 61 and S1). Other graphs could have been chosen (and were tested in a sensitivity analysis), but  
 62 led to comparable qualitative results. Ours were a compromise between over-detailed and  
 63 over-simplified descriptions. Simplified five-node ecosystem graphs were built only to  
 64 explain the influences of the rules (Fig. 1b).

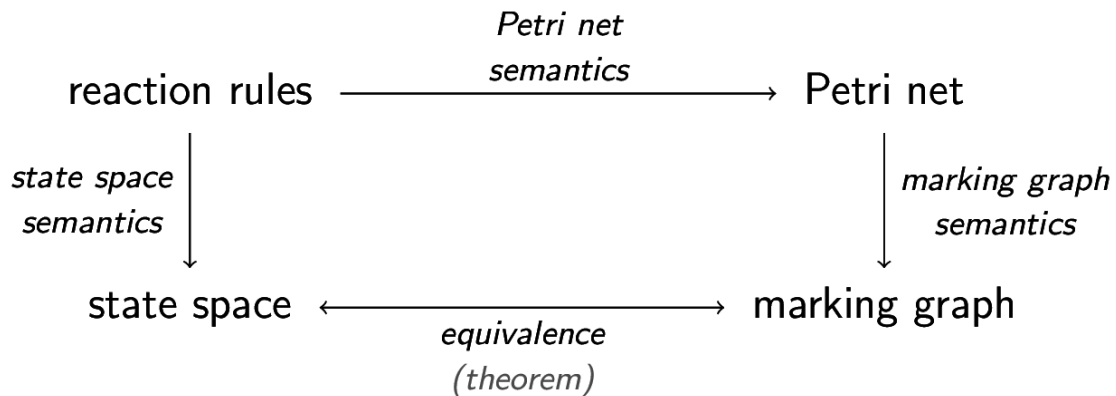
65

## 66 Appendix 2: Proof of theorem 1

67

68 In this section, we intend to prove theorem 1, which posits that the state space of  $(\mathbb{E}, s_0, R)$   
 69 is isomorphic to the marking (or reachability) graph of  $(S, T, W, M)$  (Fig. S1). This procedure  
 70 is a common way of proceeding, although never done in the specific case of our two  
 71 semantics (Best, Devillers & Koutny 2001). First, we prove that the initial state and initial  
 72 markings are equivalent. A state  $s \subseteq \mathbb{E}$  corresponds exactly to the marking  $\{e^+ \mid e \in s\} +$   
 73  $\{\bar{e} \mid e \in \mathbb{E} \setminus s\}$ , and conversely, the marking  $M$  corresponds to the state  
 74  $\{e \in \mathbb{E} \mid M(e^+) = 1\}$ . We note by  $M(s)$  the marking that corresponds to state  $s$ . From item  
 75 1 in the definition of the Petri net semantics (see main text and Fig. S1), it follows that the  
 76 initial marking is  $M(s_0)$ .

77



78

79 *Figure S1. Diagram explaining the rigorous relationships between the various semantics*  
 80 *involved in the study, and highlighting the equivalence between the marking graph and the*  
 81 *computed state space.*

82

83 We now prove that the state space and marking graph are constructed by two equivalent  
 84 inductions. To do so, we must prove that  $s \xrightarrow{r} s'$  in the reaction rules correspond to the Petri  
 85 net firing of  $M(s)[t_{r'}]M(s')$  for some transition  $t_{r'}$  such that  $r'$  is a normalized rule  
 86 obtained from  $r$ . There is an exact correspondence between normalized rules and  
 87 transitions, so that we may equivalently use one or the other.

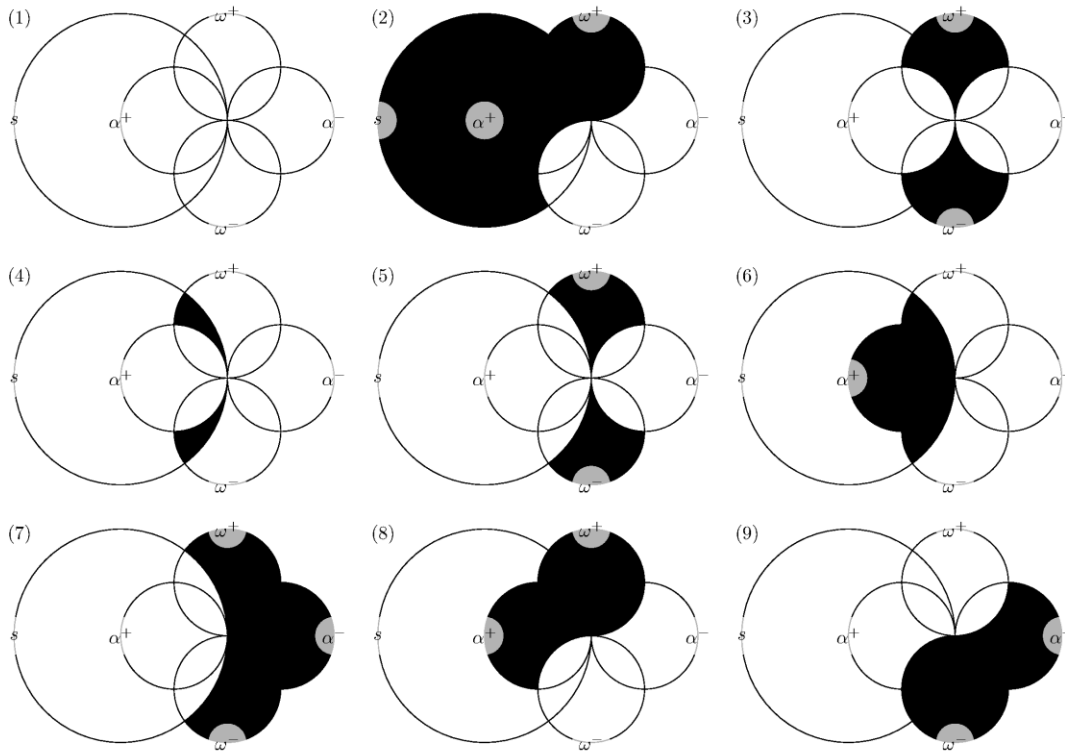
88 Let us first consider that we have  $s \xrightarrow{(\alpha^+, \alpha^-, \omega^+, \omega^-)} s'$ , and adopt the same notations  $\alpha$ ,  $\omega$ , and  
 89  $\chi$ , as in the definition of normalized rules, and set  $y \stackrel{\text{def}}{=} \chi \setminus x$ . From the definition of firing

90 rules, we have  $\alpha^+ \subseteq s$  and  $\alpha^- \cap s = \emptyset$  and  $s' \stackrel{\text{def}}{=} s \setminus \omega^- \cup \omega^+$ . From the definition of  
 91 reaction rules, we also have  $\alpha^+ \cap \alpha^- = \omega^+ \cap \omega^- = \emptyset$ . All together, these constraints yield  
 92 the Venn diagram (Fig. S2, diagram 1), while diagram 2 (Fig. S2) shows  $s'$ . Applying the two  
 93 steps of rule normalization, we see that  $r$  is transformed into  $r' \stackrel{\text{def}}{=} (\alpha^+ \cup x, \alpha^- \cup y, \omega^+ \cup$   
 94  $((\alpha^+ \cup x) \setminus \omega), \omega^- \cup ((\alpha^- \cup y) \setminus \omega)$ . We, show  $\chi$  in diagram 3 and take the partition  $x \sqcup$   
 95  $y$  such that  $x$  corresponds to diagram 4 and  $y$  corresponds to diagram 5 (Fig. S2). We can  
 96 now verify that:

- 97 •  $r'$  is enabled because:
- 98 ○  $\alpha^+ \cup x$ , depicted as diagram 6, is a subset of  $s$ ,
  - 99 ○  $\alpha^- \cup y$ , depicted as diagram 7, does not intersect  $s$ ;
- 100 •  $s \xrightarrow{r'} s'$  because:
- 101 ○ let  $p \stackrel{\text{def}}{=} \omega^+ \cup ((\alpha^+ \cup x) \setminus \omega)$  as depicted in diagram 8,
  - 102 ○ let  $q \stackrel{\text{def}}{=} \omega^- \cup ((\alpha^- \cup y) \setminus \omega)$  as depicted in diagram 9,
  - 103 ○ we have  $s' = (s \setminus q) \cup p$ .

104 Conversely, we can prove with exactly the same diagrams and a mirrored reasoning that if  $s$   
 105  $\xrightarrow{r'} s'$ , then we also have  $s \xrightarrow{r} s'$ . □

106



107

108

109 Figure S2. The distinct sets involved in the firing of a reaction rule  $s \xrightarrow{(\alpha^+, \alpha^-, \omega^+, \omega^-)} s'$ .

110

111 In addition, firing a rule independently to some others often leads to unrealistic paths (e.g.  
 112 removing water without removing fishes in it). Therefore, we defined a new kind of rules  
 113 called constraints, preventing the model from simulating such unrealistic paths. Constraints  
 114 have a condition and a realization part, just as rules *stricto sensu* do, and model inevitable

115 (mandatory) events given the system state. The sole difference between rules and  
116 constraints is that constraints have priority on rules *stricto sensu*. In the prey-predator  
117 system, the system state S1 is unrealistic; so, the rule R2 has to be transformed into a  
118 constraint (C1: N-, P+  $\rightarrow$  P-). From a given state, the model first computes all trajectories  
119 opened up by the defined constraints and then only, when all the system states obtained are  
120 realistic (i.e. there is no longer any enabled constraint), the enabled rules are fired. In brief,  
121 the discrete models proposed here is qualitative, mechanistic (processes are explicit),  
122 deterministic (no stochasticity) and asynchronous (all rules are applied as soon as possible,  
123 no rule conflict as they systematically branch in the state space).

### 125 Appendix 3: State-space refined analyses

126  
127 The termite ecosystem model combines one initial state, two strongly connected  
128 components (SCC) and four main deadlocks (Fig. 4). We may zoom into the SCC B' graph (Fig.  
129 S3a), as well as simplify it by merging each distance to exit (DTX) class into one new node to  
130 observe which rule allows moving from one class to another (Fig. S3b). The DTX class 0, only,  
131 is a SCC, while the other DTX classes are not strongly connected. For this reason, to merge  
132 the other classes may create paths that are not realizable in the modeled system. On this  
133 merged graph, hexagonal-shape nodes are those that contain at least one entrance of the  
134 SCC, while nodes are labeled with the DTX in parentheses to denote that this is a merged  
135 node.

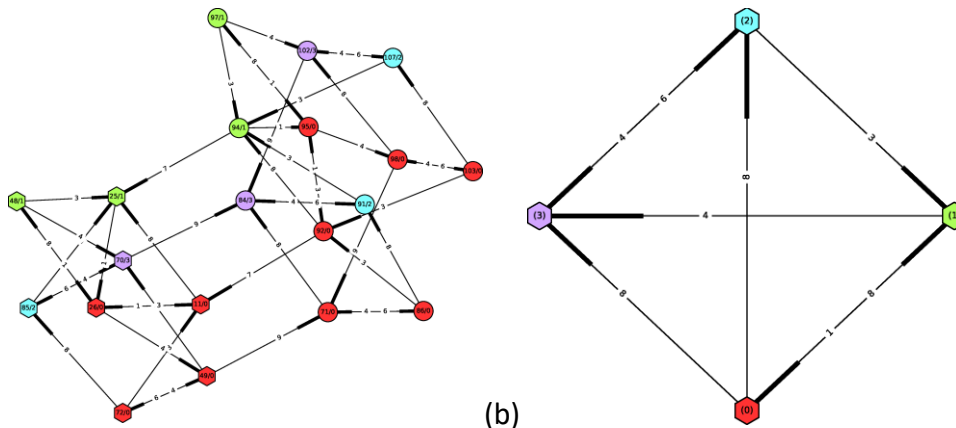
136 Leaving DTX class 0 is always done through rule 8, while returning to class 0 is always done  
137 by decrementing DTX by one unit. Moreover, decreasing the DTX is always done using the  
138 same rules as shown by path (3)  $\xrightarrow{6}$  (2)  $\xrightarrow{3}$  (1)  $\xrightarrow{1}$  (0). Finally, this merged graph is not  
139 complete: moving from a DTX class  $x$  to a class  $y > x$  is easier (*i.e.*, there are more paths to  
140 do so) than moving in reverse ( $x < y$ ). So, as a second observation on the paths in our  
141 termite model, the system will eventually reach a deadlock if it executes a sequence  
142 finishing with 6, 3, 1, and then 12 or 13 (in this order, but possibly interleaved with other  
143 rules). From SCC B, we can make the same observation, except that the system may execute  
144 rule 11 to reach SCC B'. As a third observation, a random path within SCC B or B' is more  
145 likely to go through classes with higher DTX.

146 More details of the termite system behavior are available by removing all the edges  
147 between nodes of DTX class 0, because class 0 is a SCC (we thus know that every node can  
148 be reached from another within this DTX class) (Fig. S3a). It appears that DTX class 2 is not  
149 connected and contains only transient states from which the system reaches DTX 1 or 3.  
150 Moreover, the longest path within DTX class 1 is  $97 \rightarrow 94 \rightarrow 25$ , and within DTX class 3 it is  
151  $102 \rightarrow 84$  or  $70 \rightarrow 84$ . Therefore the system cannot stay for a long period without changing  
152 its DTX value. As a fourth observation, the system can stay within the same DTX class for  
153 short runs only: three successive states for DTX 1, one state for DTX 2, two states for DTX 3.

154 Although the system can reach any other class from DTX 0, leaving DTX 0 is always done  
155 through rule 8 (Fig. S3b). As a fifth observation, the only way to increase DTX in SCC B', and  
156 thus to postpone the collapse, is to fire rule 8. In addition, we observe that: i) a random path  
157 within any SCC (B' or B) is more likely to move through classes with higher DTX; ii) the  
158 system can stay within the same DTX class for short runs only; and iii) the only way to

159 increase DTX in SCC B', and thus to postpone the system collapse, is to fire rule 8. Finally, the  
 160 model allows for accurate identification of the (simple, i.e. non-looping) trajectories of the  
 161 system within each SCC.

162 Moreover, the largest SCC within this graph consists in all the states with non-zero DTX plus  
 163 states 26 and 95. Removing any of these two latter states also destroys the SCC B'. Hence,  
 164 these states play central roles within SCC B' when we focus on paths trying to avoid DTX 0.  
 165 Finally, small SCCs composed of two states only may also be found: {70, 85}, {84 – 91}, and  
 166 {102, 107}. This means that avoiding DTX 0 is not possible on arbitrarily long trajectories  
 167 without ultimately repeating these paths, yet with infinite runs alternating the two states of  
 168 each couple. However, we may find an infinite number of paths without such oscillating  
 169 paths that stay with DTX 0 for only one state (either 26 or 95).



170 (a) 171 (b)  
 172 *Figure S3. Zoom of the SCC B' (a) of the state-space (Fig. 4a), and a simplified version (b) in*  
 173 *which each distance to exit (DTX) class has been merged into a single node. Here, nodes and*  
 174 *interactions outside SCC B' have been hidden. Hexagonal-shaped nodes are those from which*  
 175 *the system enters the SCC (8 possible states here). Nodes are labelled with pairs n/d where d*  
 176 *and the color represent the distance to an exit node (DTX) of the focus state, that is, a state*  
 177 *from which a rule may push the system outside the SCC (towards a deadlock, Fig. 4). In the*  
 178 *simplified SCC (b), nodes are labelled with DTX and highlighted on both figures with a specific*  
 179 *color (DTX=0 in red, 1-green, 2-cyan and 3-purple).*

181 The simplified and trajectory-based version of the state space is informative too (Fig. 4b).  
 182 From the SCC B, the system can reach SCC B' with rule 11 only (i.e. killing ant competitors),  
 183 or the system can reach deadlock by first executing rule 12 (ants kill termites) or rule 13 (lack  
 184 of air kills termites). From SCC B', rule 13 only remains possible because ant competitors are  
 185 absent in the system. After one of these rules has pushed the system from any of its SCCs,  
 186 several paths are available and correspond to the progressive depletion of resources in the  
 187 system, which we may observe by plotting the paths (not depicted here). As a sixth and last  
 188 observation for the termite system, the system dies if and only if it fires rule 12 or 13 (lack of  
 189 reproductives or of fresh air, Table 2). Then, depending on the state from which this decisive  
 190 rule is fired, the system executes four time steps (four rules) at most before collapsing.  
 191 These results are contingent on the termite system modeled, but any (eco)system would  
 192 benefit from this model ability to identify the decisive rules or sequences of rules and to  
 193 quantify the dynamics associated with specific collapse or "alive" states (SCC).

194

195 **References**

196

197 Best, E., Devillers, R. & Koutny, M. (2001) *Petri Net Algebra*. Springer, Berlin.

198 Engel, M.S. & Krishna, K. (2004) Family-Group Names for Termites (Isoptera).

199 *American Museum novitates*, **3432**, 9.

200 Giavitto, J.L. & Michel, O. (2003) Modeling the topological organization of cellular  
201 processes. *Biosystems*, **70**, 149-163.

202 Godin, C. (2000) Representing and encoding plant architecture: A review. *Annals of*  
203 *Forest Science*, **57**, 413-438.

204 Hyodo, F., Inoue, T., Azuma, J.I., Tayasu, I. & Abe, T. (2000) Role of the mutualistic  
205 fungus in lignin degradation in the fungus-growing termite *Macrotermes*  
206 *gilvus* (Isoptera; Macrotermitinae). *Soil Biology and Biochemistry*, **32**, 653-  
207 658.

208 Jaffe, K., Ramos, C. & Issa, S. (1995) Trophic interactions between ants and termites  
209 that share common nests. *Annals of the Entomological Society of America*, **88**,  
210 328-333.

211 Leal, I.R. & Oliveira, P.S. (1995) Behavioral ecology of the neotropical termite-  
212 hunting ant *Pachycondyla* (Termitopone) *marginata*: colony founding, group-  
213 raiding and migratory patterns. *Behavioral Ecology and Sociobiology*, **37**,  
214 373-383.

215 Noirot, C. (1955) *Recherches sur le polymorphisme des termites supérieurs*  
216 (*Termitidae*). Masson et Cie.

217 Noirot, C. (1956) Les sexués de remplacement chez les termites supérieurs  
218 (*Termitidae*). *Insectes sociaux*, **3**, 145-158.

219 Rosengaus, R.B. & Traniello, J.F. (1991) Biparental care in incipient colonies of the  
220 dampwood termite *Zootermopsis angusticollis* Hagen (Isoptera: Termopsidae).  
221 *Journal of insect behavior*, **4**, 633-647.

222 Sayama, H. & Laramée, C. (2009) Generative Network Automata: A Generalized  
223 Framework for Modeling Adaptive Network Dynamics Using Graph  
224 Rewritings. *Adaptive Networks. Theory, models and applications* (eds T.  
225 Gross & H. Sayama), pp. 311-332. Springer, NECSI  
226 Cambridge/Massachusetts.

227 Shellman-Reeve, J.S. (1990) Dynamics of biparental care in the dampwood termite,  
228 *Zootermopsis nevadensis* (Hagen): response to nitrogen availability.  
229 *Behavioral Ecology and Sociobiology*, **26**, 389-397.

230 Shellman-Reeve, J.S. (1997) Advantages of biparental care in the wood-dwelling  
231 termite, *Zootermopsis nevadensis*. *Animal Behaviour*, **54**, 163-170.

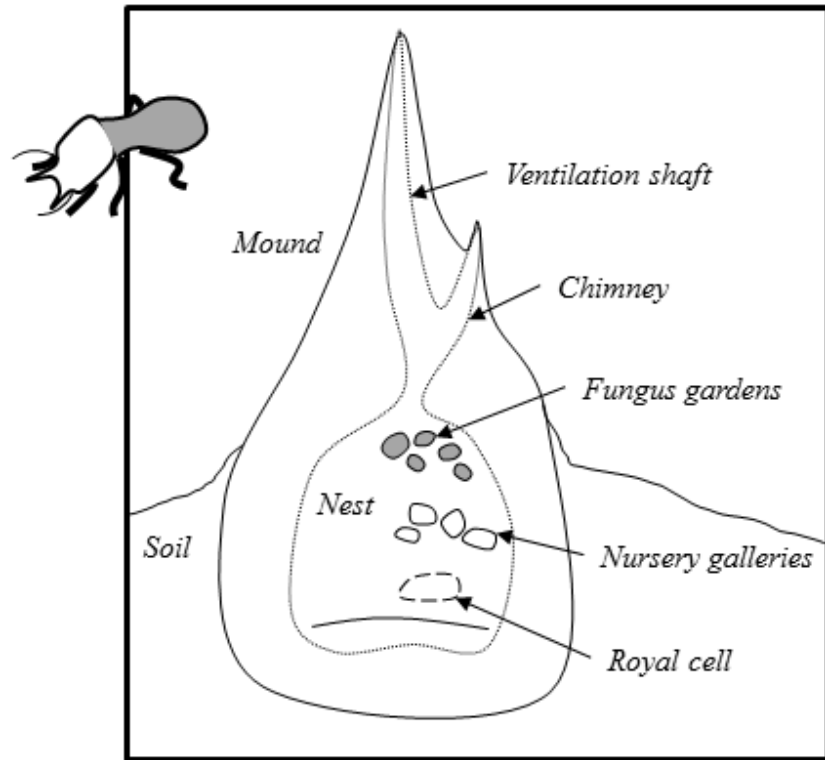
232 Thomas, R. & Kaufman, M. (2001) Multistationarity, the basis of cell differentiation  
233 and memory. II. Logical analysis of regulatory networks in terms of feedback  
234 circuits. *Chaos*, **11**, 180-195.

235 Turner, J.S. (2009) *The extended organism: the physiology of animal-built structures*.  
236 Harvard University Press.

237

238

a)



b)

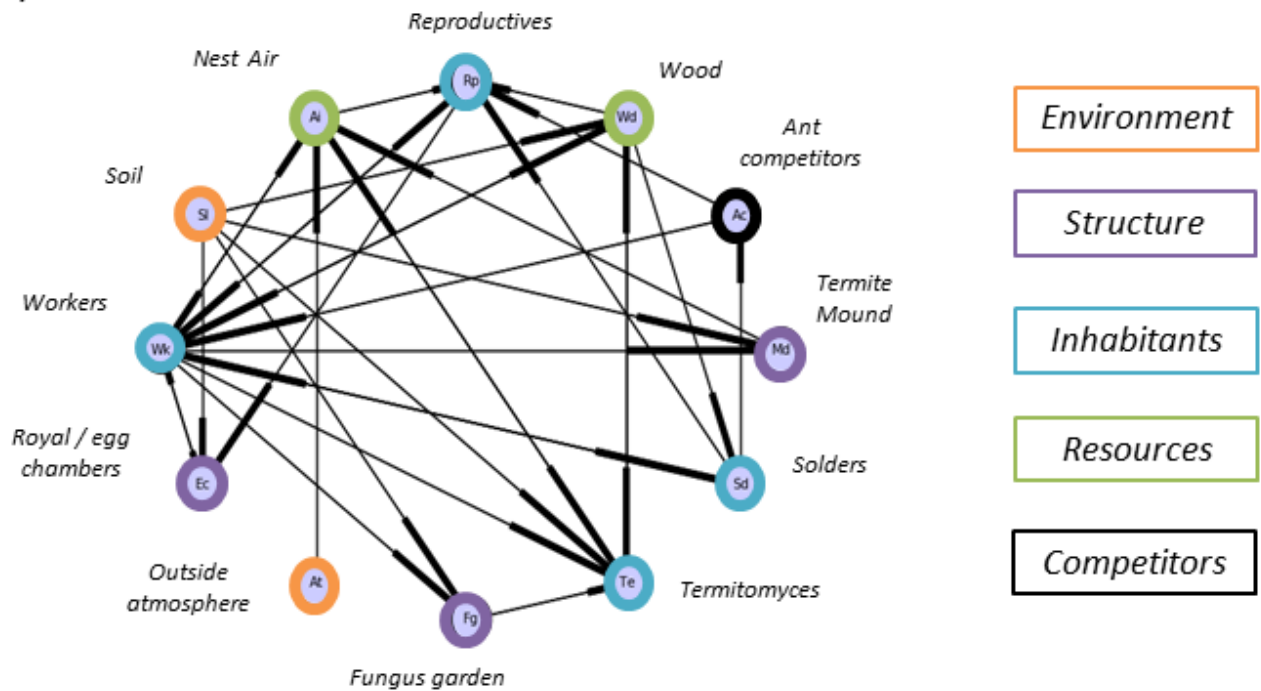


FIGURE 1

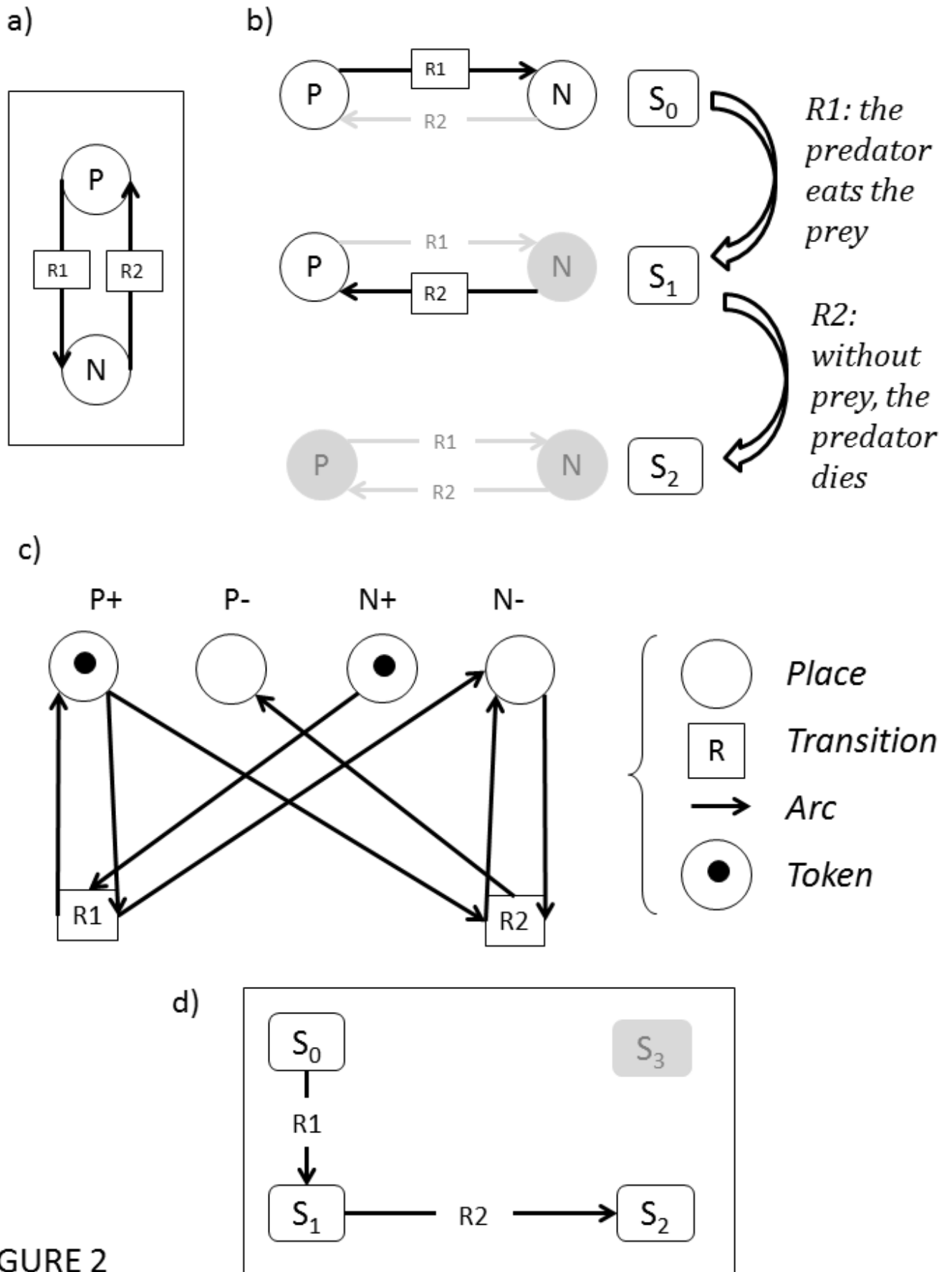
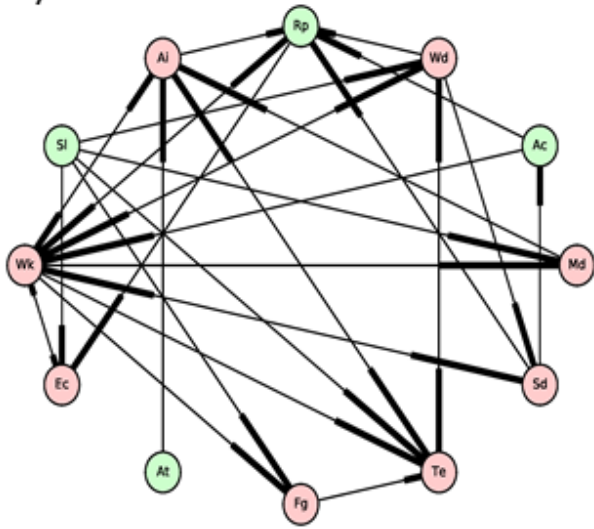
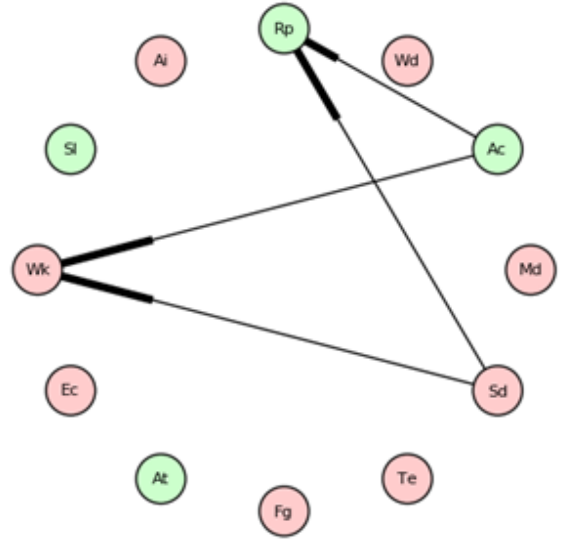


FIGURE 2

a)



12:  $Ac^+, Sd^- \rightarrow Wk^-, Rp^-$



b)

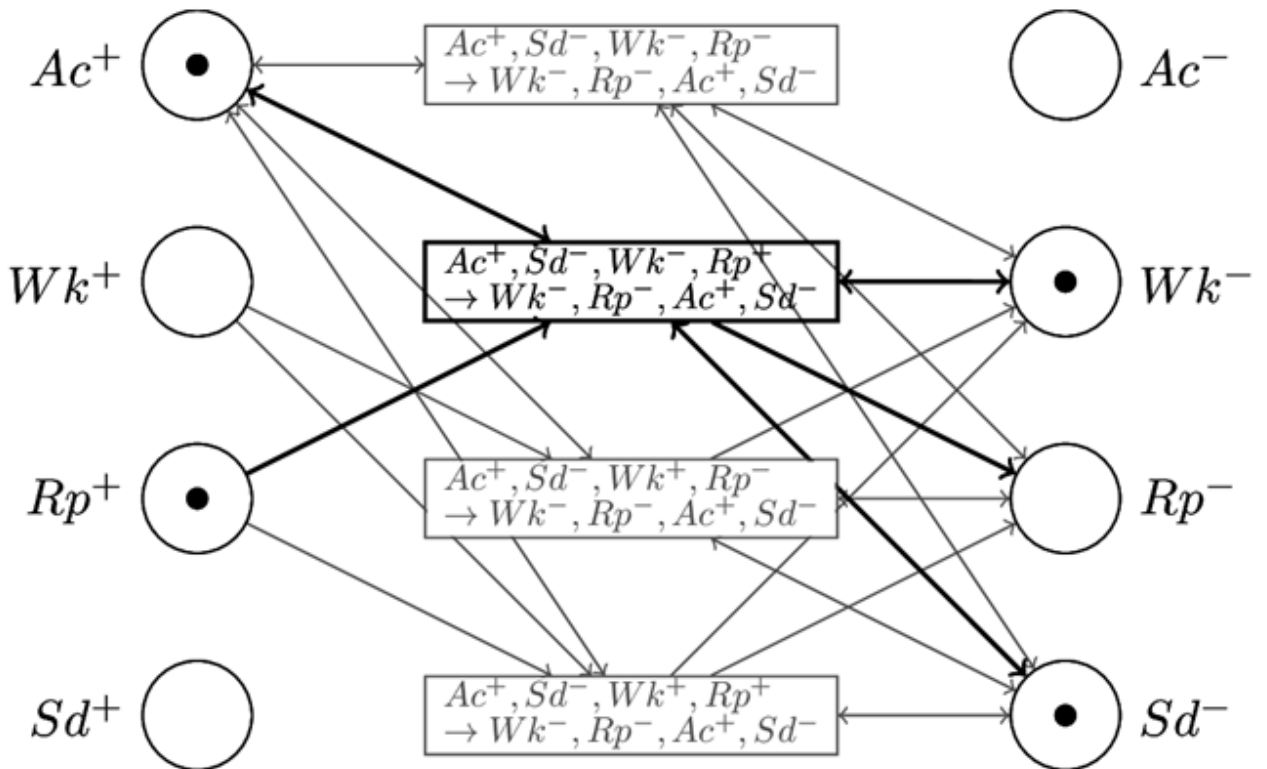


FIGURE 3

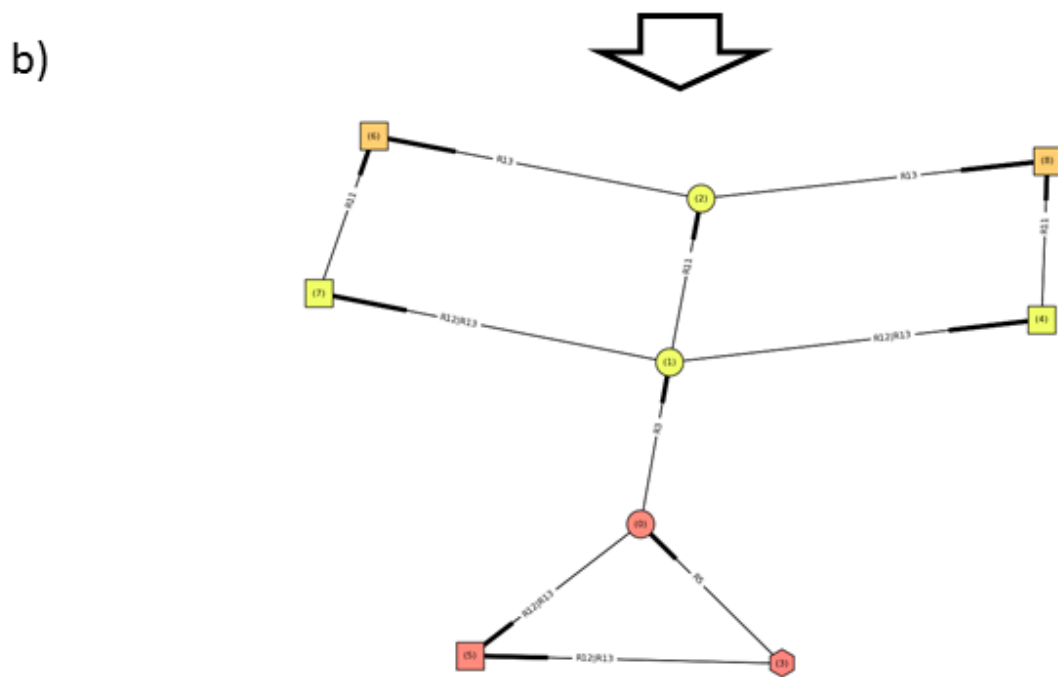
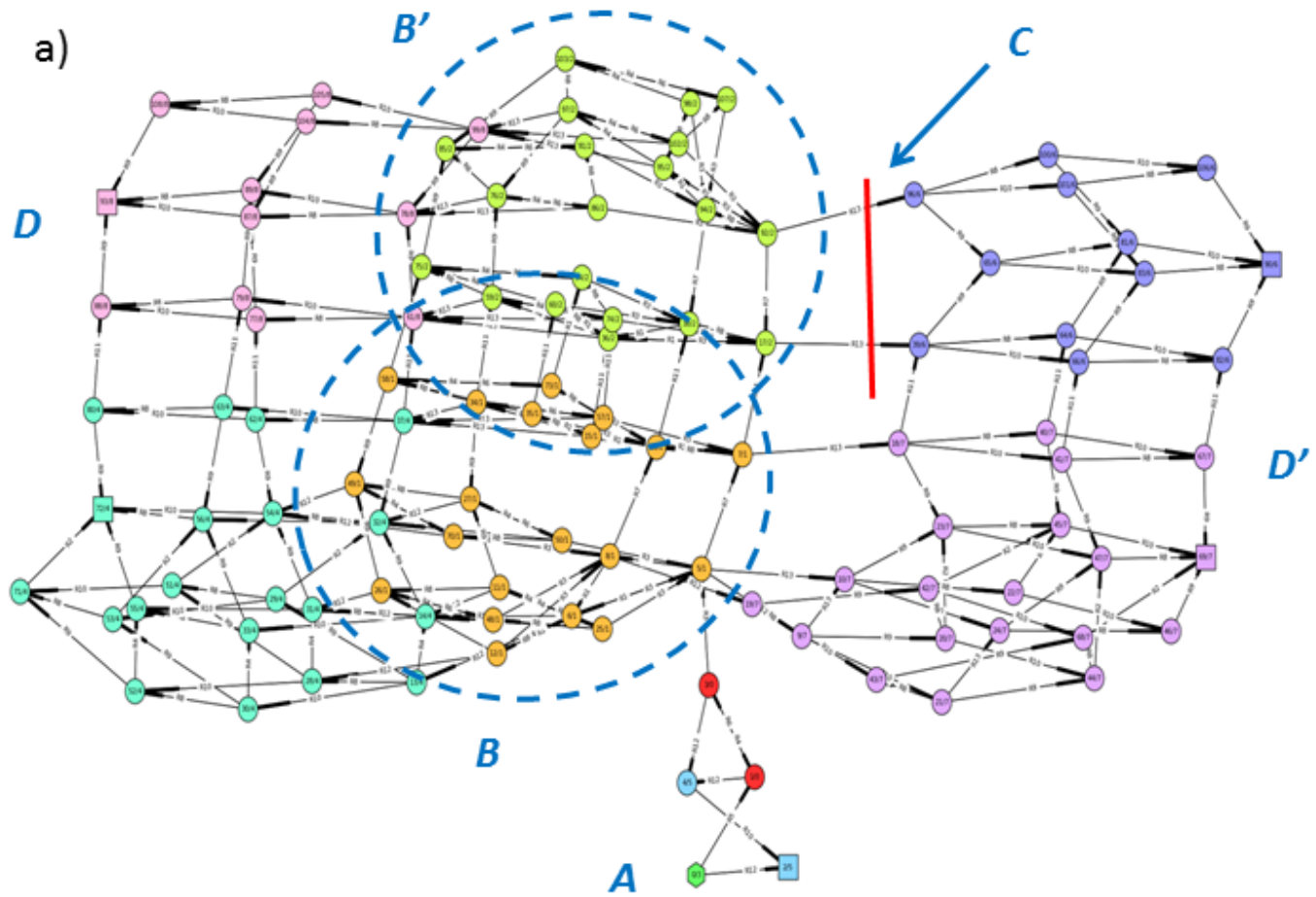


FIGURE 4